Time of Emergence Large Ensemble Intercomparison for Ocean Biogeochemistry

" ToE-LE-MIP"

Sarah Schlunegger

& Keith B. Rodgers, Jorge L. Sarmiento, Tatiana Ilyina
John Dunne , Yohei Takano, James Christian, Mathew Long
Thomas L. Frölicher, Richard Slater, Flavio Lehner

Large Ensemble Workshop | NCAR
July 26th, 2019

Outline

Ocean Carbon Cycle 101
Time-of-Emergence Diagnostic
Results

Time of Emergence

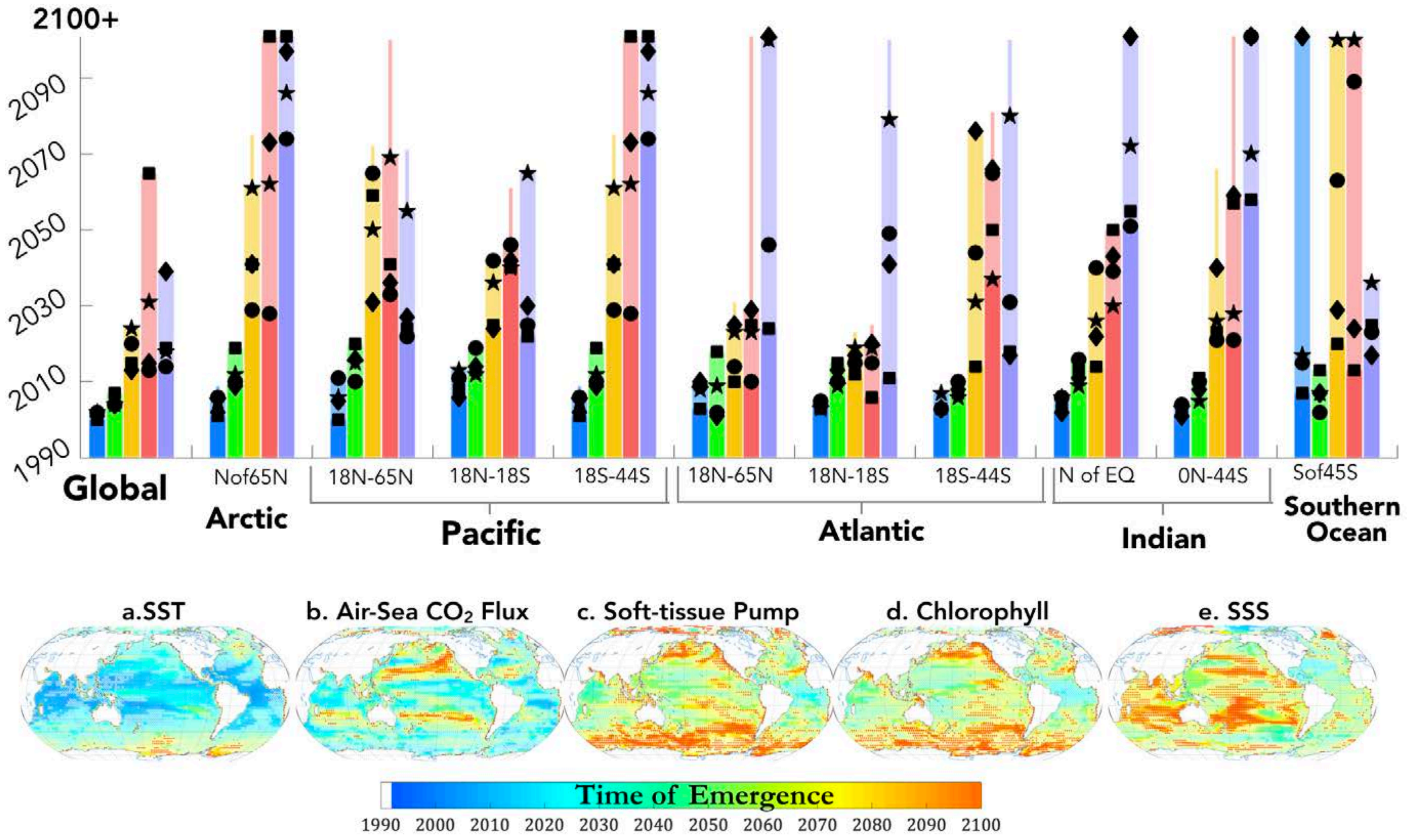

Partitioning Uncertainty

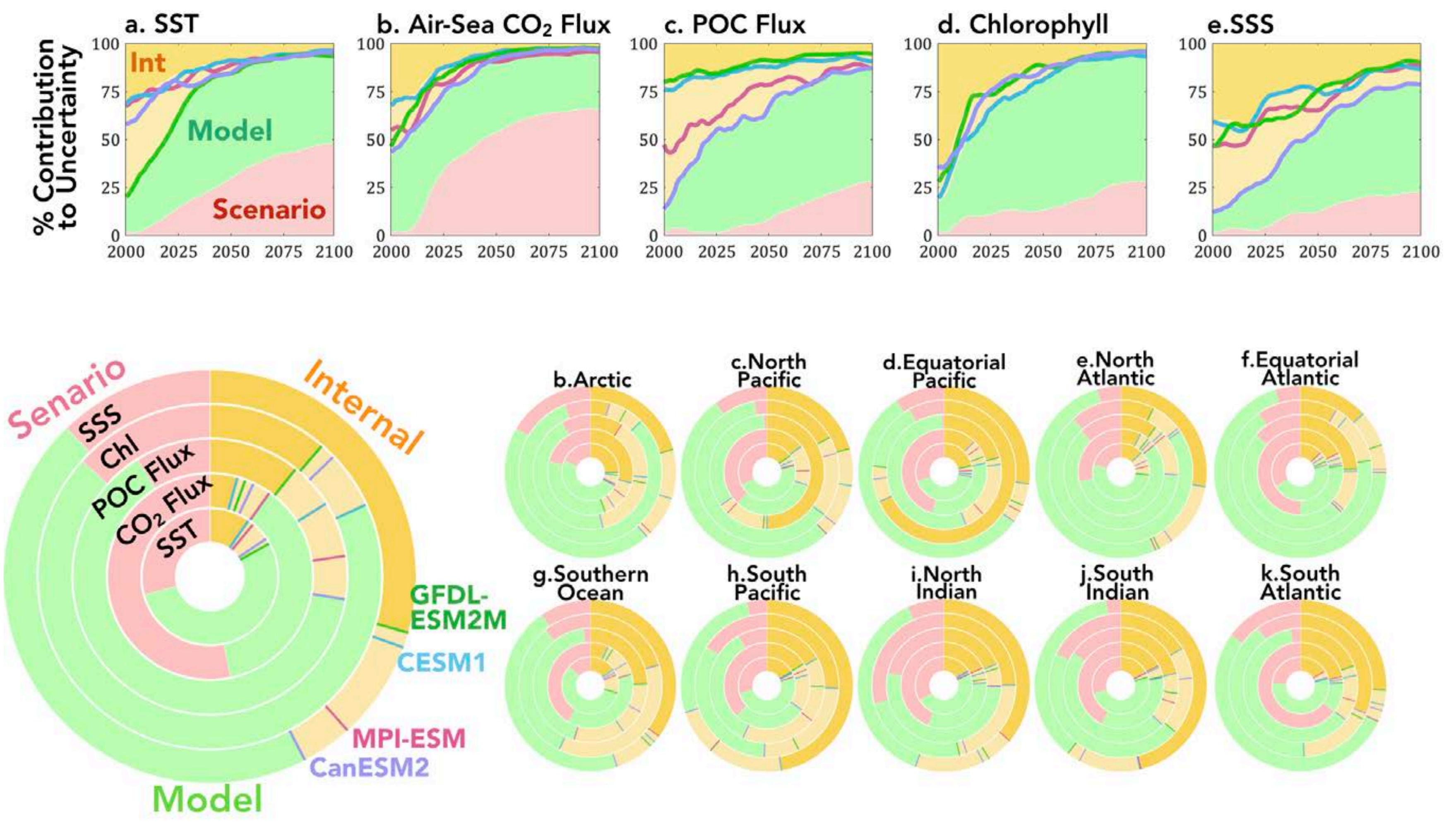

Contemporary ocean carbon and heat sink

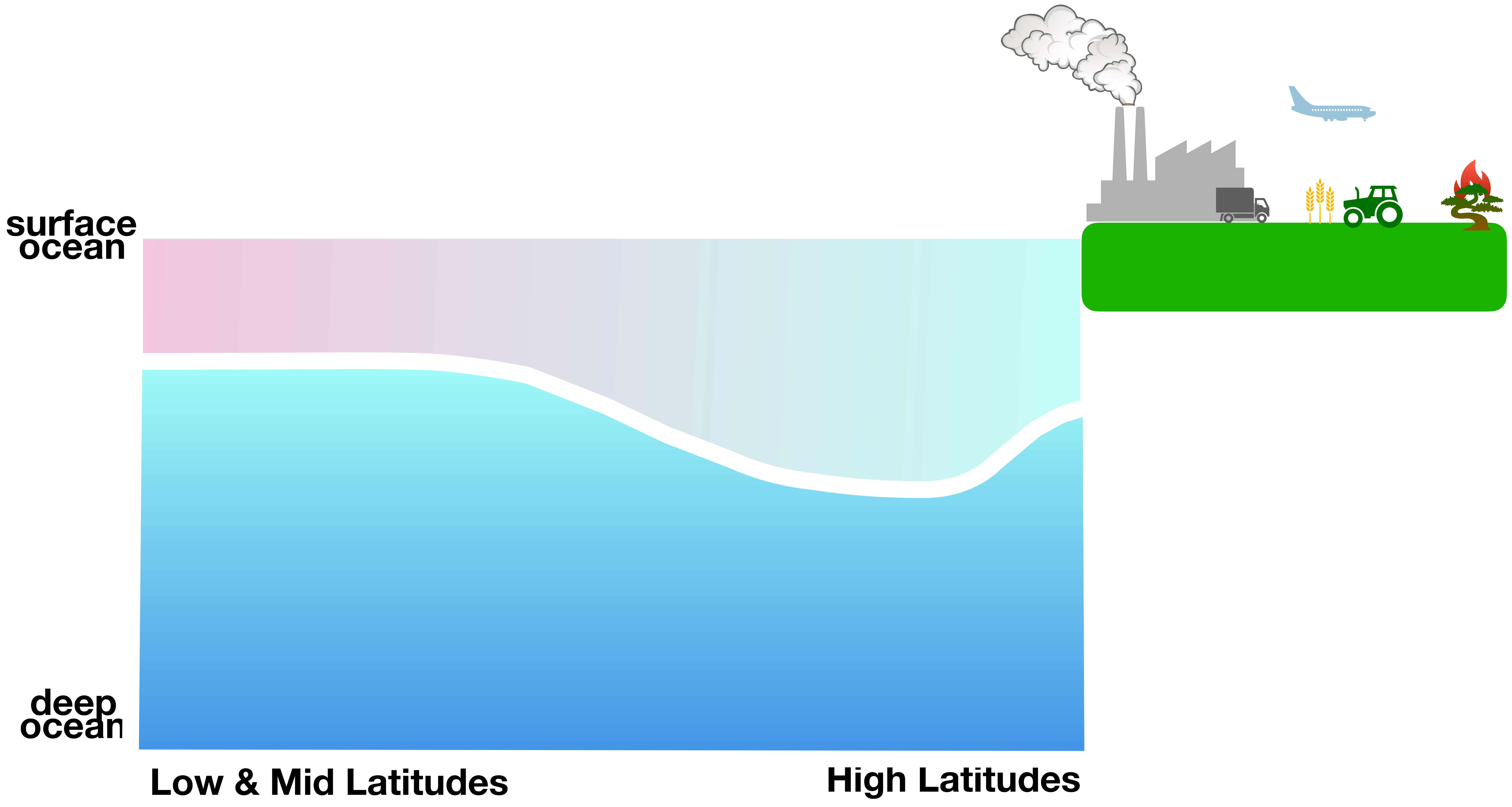

Contemporary ocean carbon and heat sink

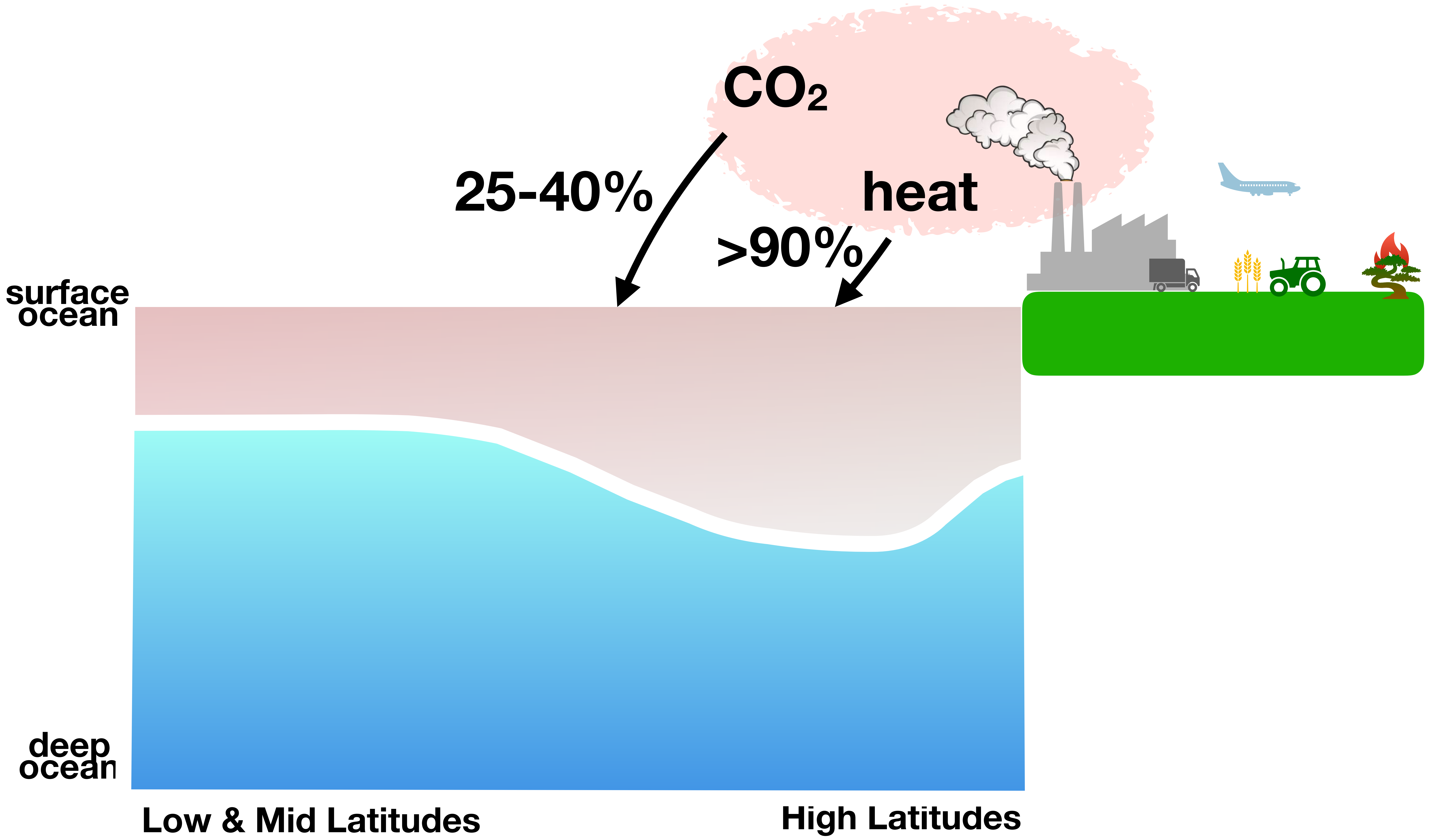

Schematic of ocean carbon cycle

Pumps transport carbon to deep ocean

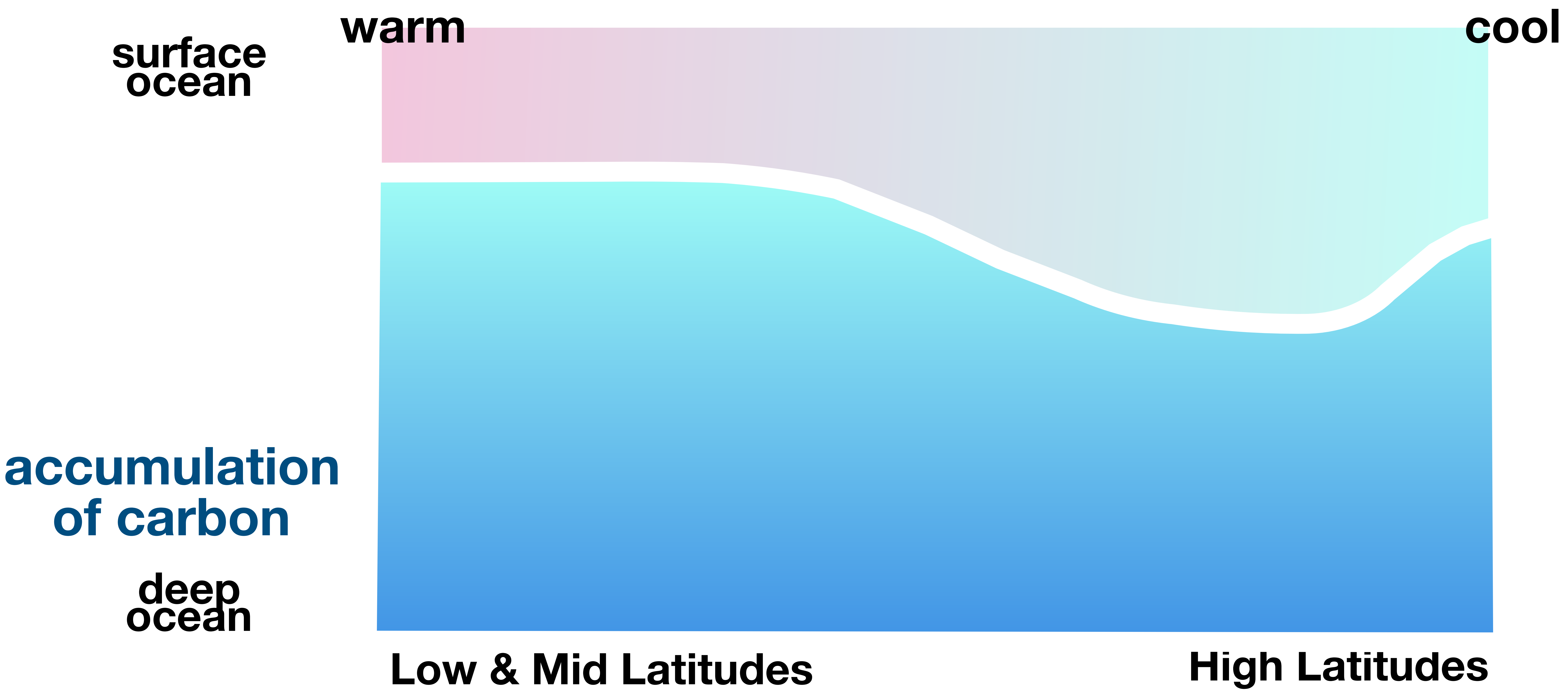

Schematic of ocean carbon cycle

Pumps transport carbon to deep ocean

1. solubility pump 2. biological pumps

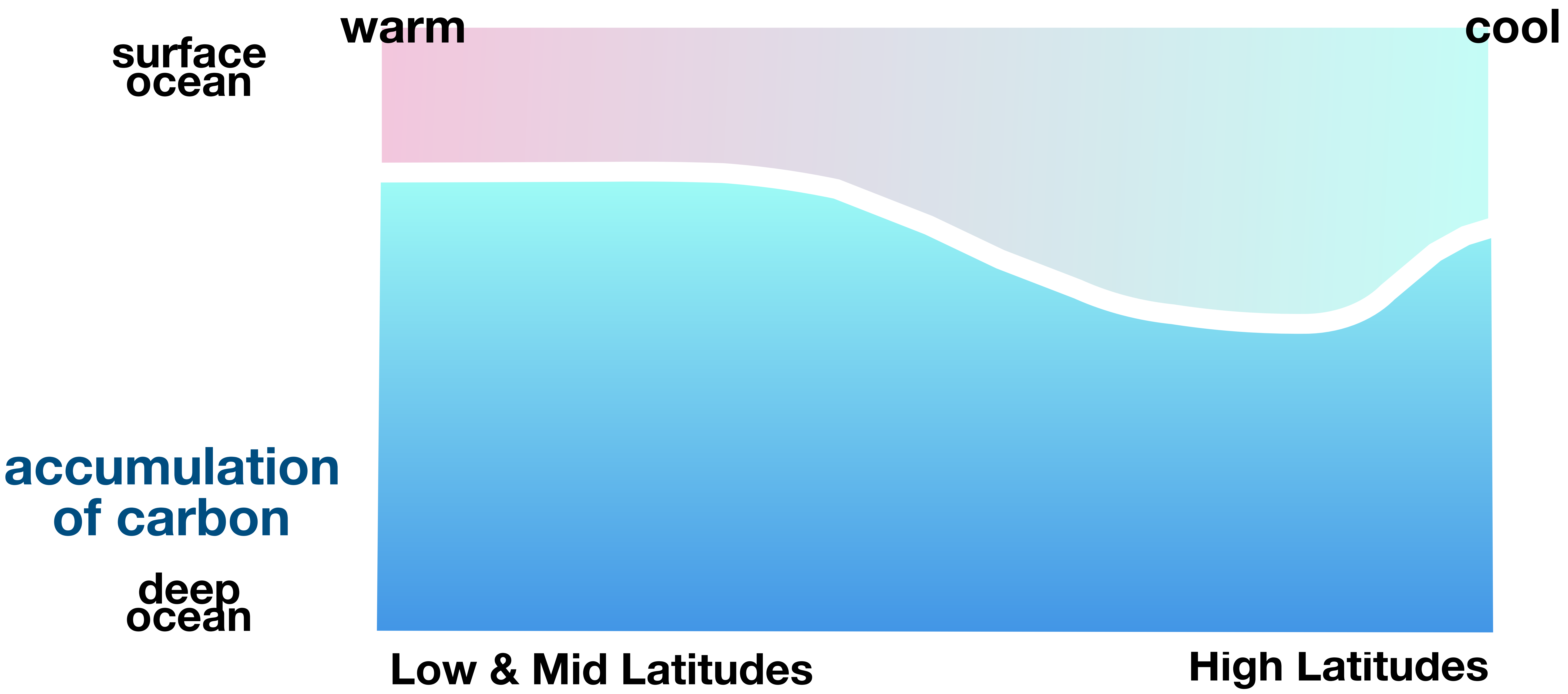

Schematic of ocean carbon cycle

Pumps transport carbon to deep ocean

1. solubility pump 2. biological pumps

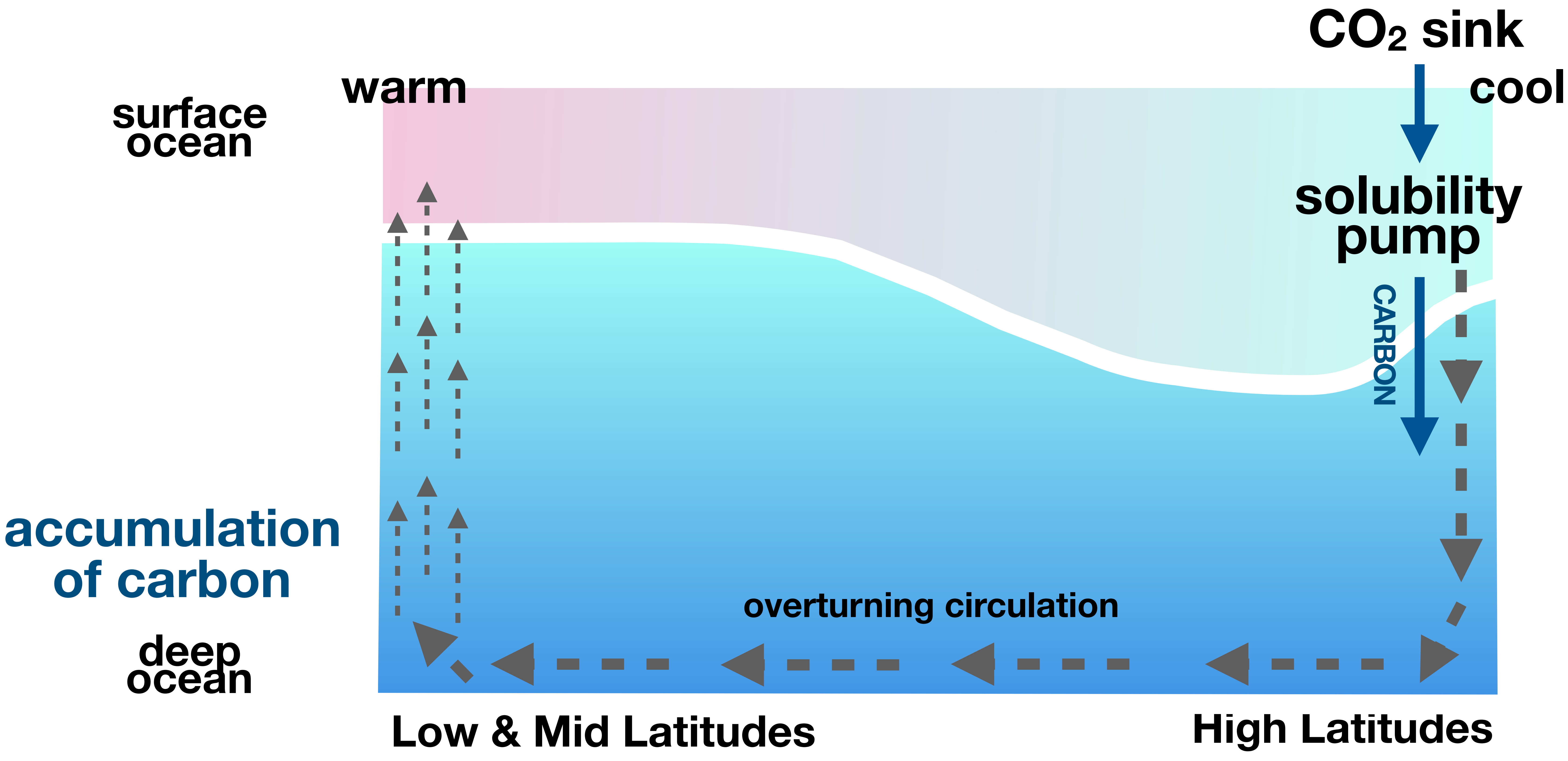

Schematic of ocean carbon cycle

Pumps transport carbon to deep ocean

1. solubility pump 2. biological pumps

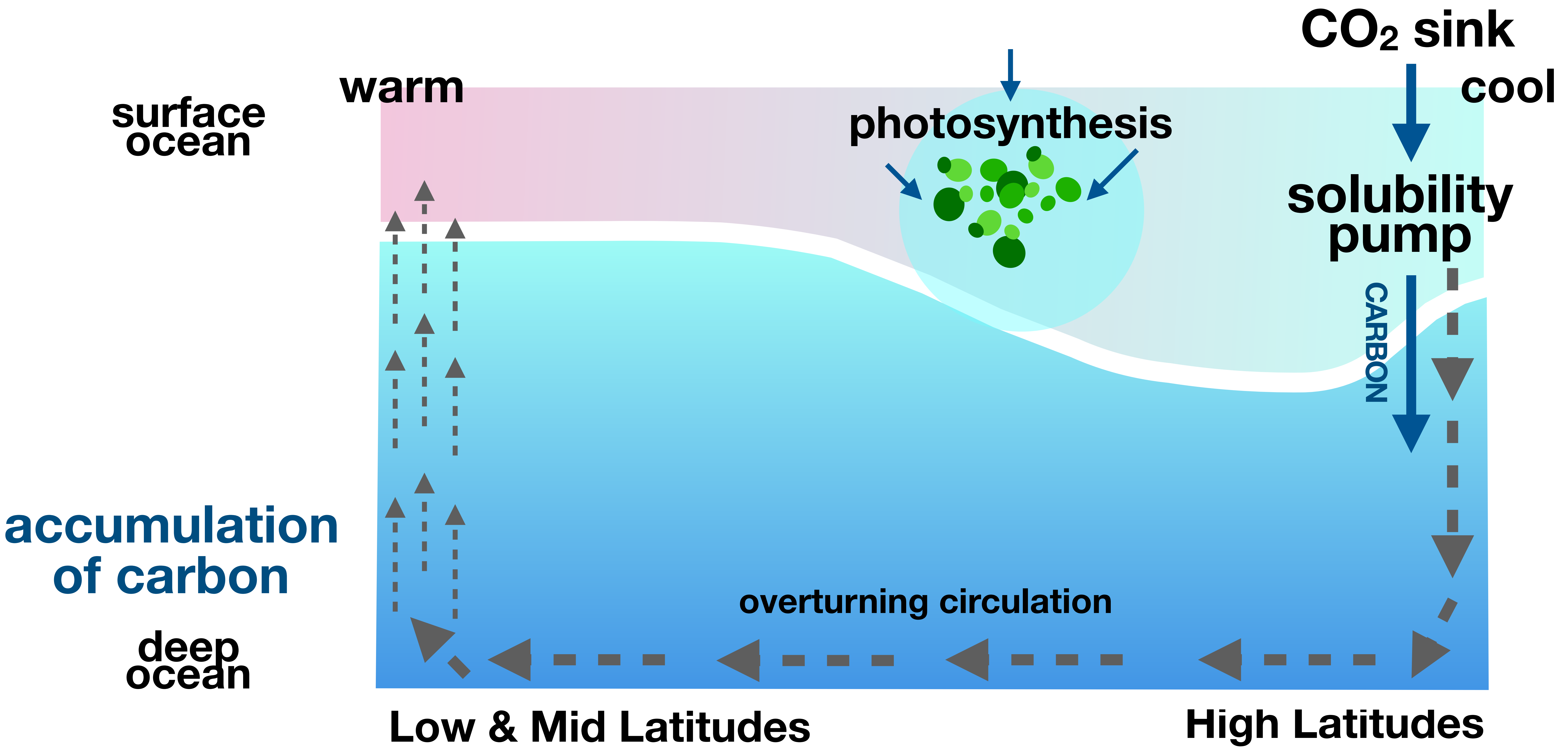

Schematic of ocean carbon cycle

Pumps transport carbon to deep ocean

1. solubility pump 2. biological pumps

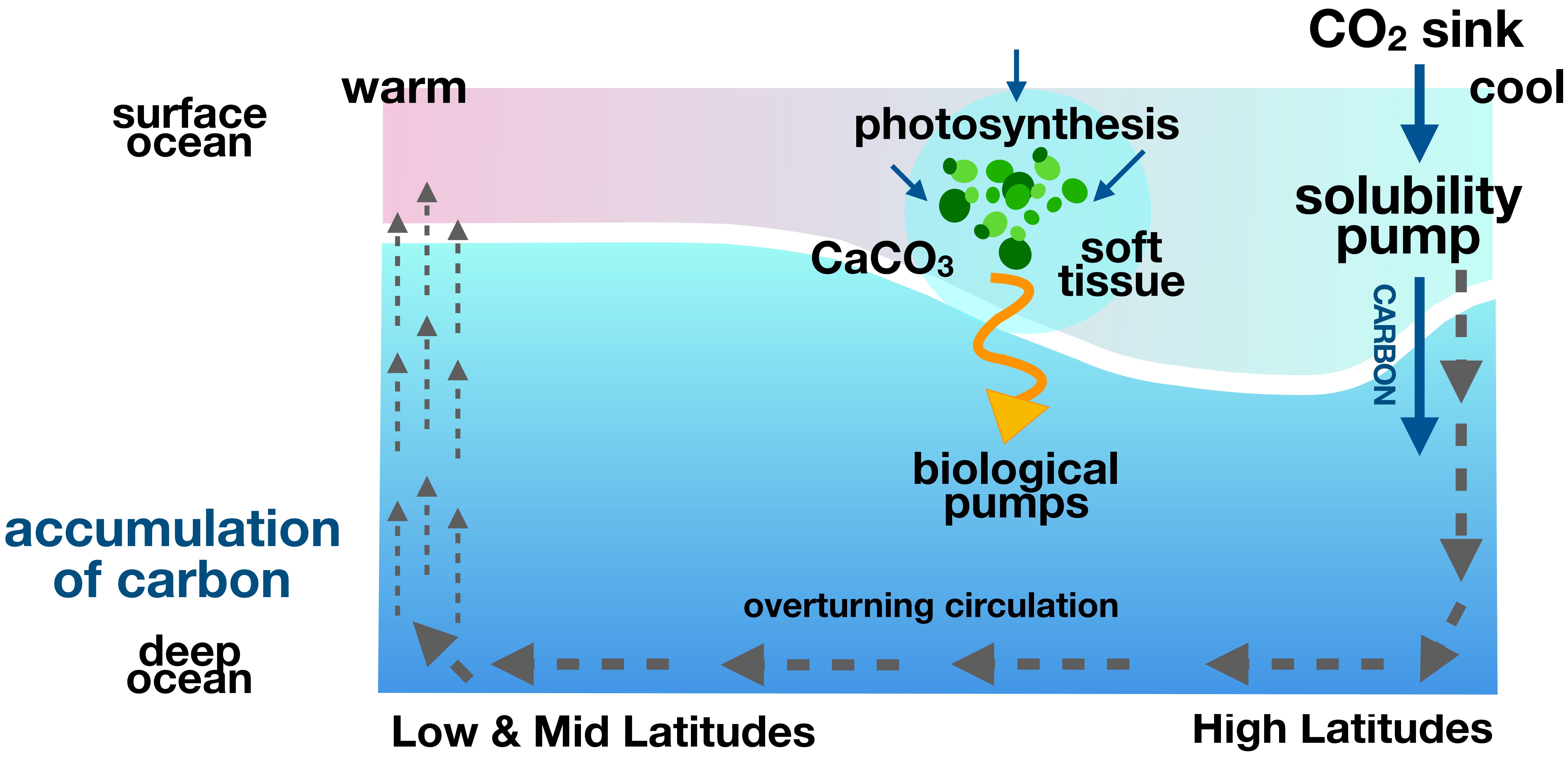

Schematic of ocean carbon cycle

Pumps transport carbon to deep ocean

Observable Variables of intrest	Temp	air-sea CO_2 flux	Organic Carbon Export @ 100m	chlorophyll	Salinity

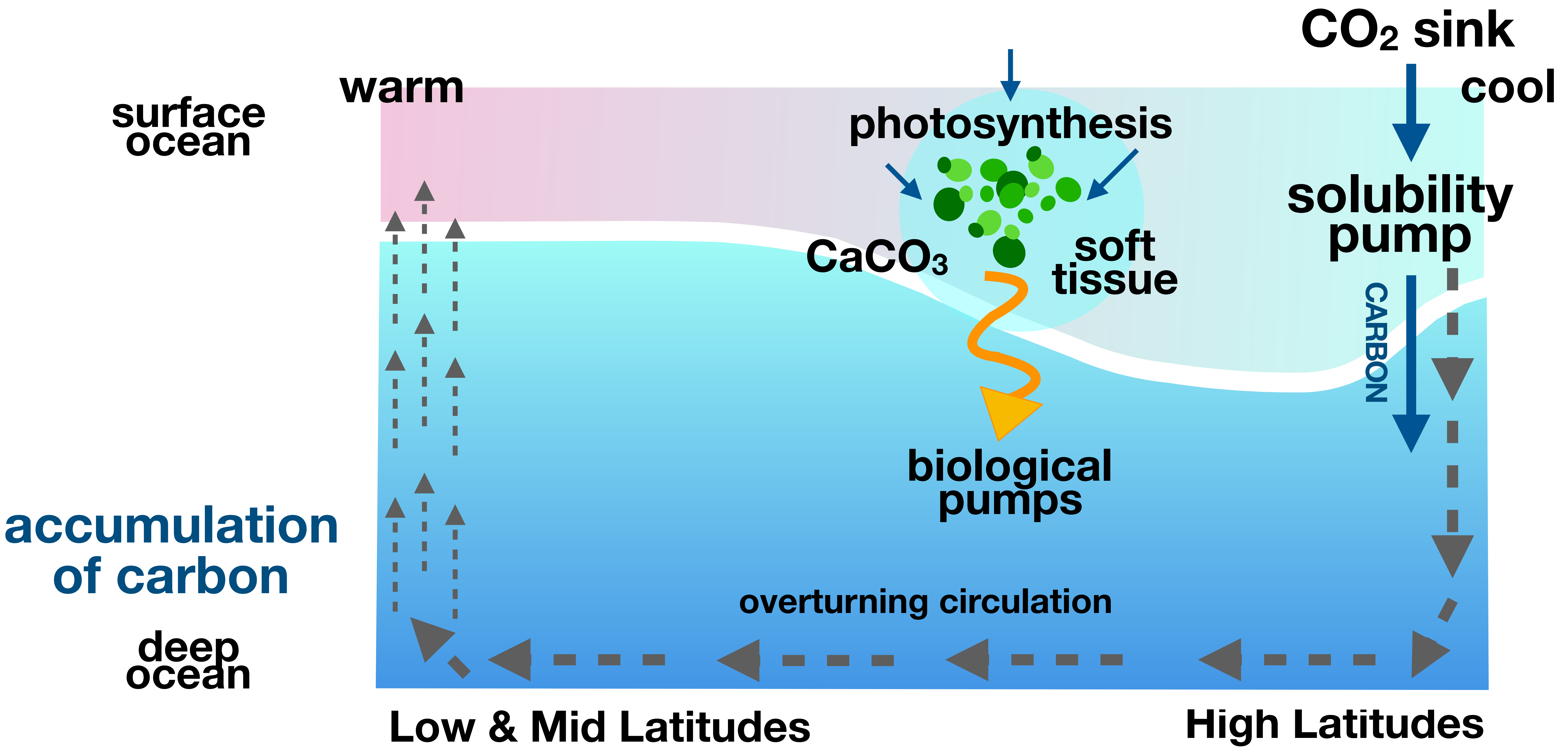

Time-of-Emergence

point in time the climate-change signal is statistically distinguishable from the noise

a multi-purpose metric

(1) inform observing system design

(2) inform impact timescales

(3) diagnostic which intelligently normalize anthropogenic responses across disparate variables

Sources of Uncertainty in Climate Observation and Simulation

Time-of-Emergence

point in time the climate-change signal is statistically distinguishable from the noise

a multi-purpose metric

(1) inform observing system design

(2) inform impact timescales

(3) diagnostic which intelligently normalize anthropogenic responses across disparate variables

Sources of Uncertainty in Climate Observation and Simulation

Time-of-Emergence

point in time the climate-change signal is statistically distinguishable from the noise

a multi-purpose metric

(1) inform observing system design

(2) inform impact timescales

(3) diagnostic which intelligently normalize anthropogenic responses across disparate variables

Sources of Uncertainty in Climate Observation and Simulation

Time-of-Emergence

point in time the climate-change signal is statistically distinguishable from the noise

a multi-purpose metric

(1) inform observing system design

(2) inform impact timescales

(3) diagnostic which intelligently normalize anthropogenic responses across disparate variables

Sources of Uncertainty in Climate Observation and Simulation

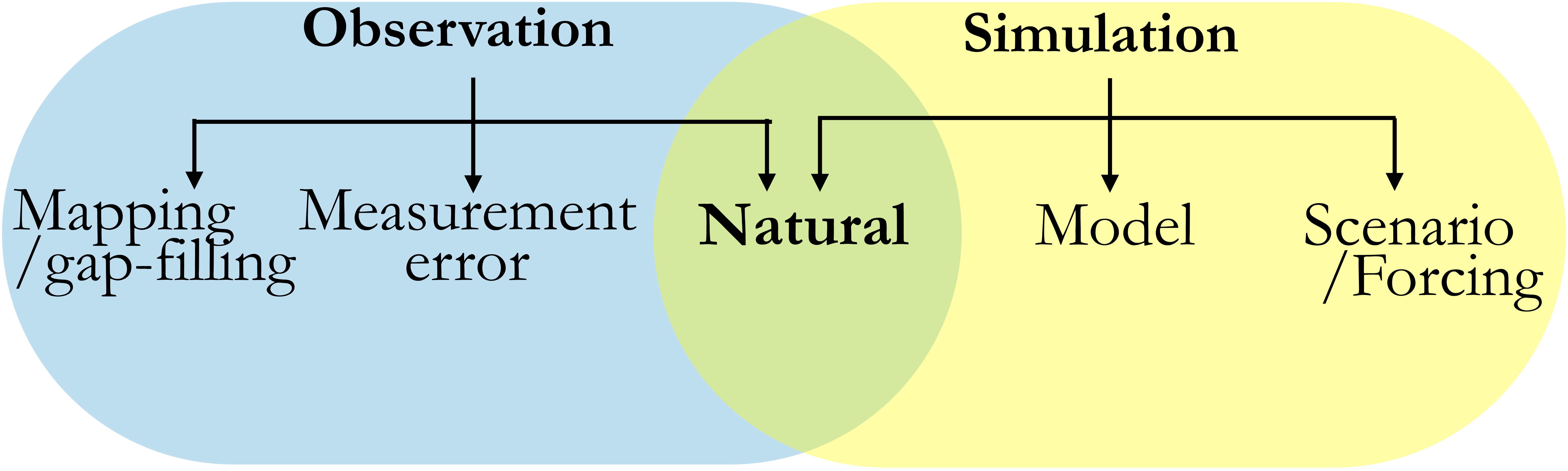

Figure from Schlunegger et al., 2019, in press

Time-of-Emergence

point in time the climate-change signal is statistically distinguishable from the noise

a multi-purpose metric

(1) inform observing system design

(2) inform impact timescales

(3) diagnostic which intelligently normalize anthropogenic responses across disparate variables

Sources of Uncertainty in Climate Observation and Simulation

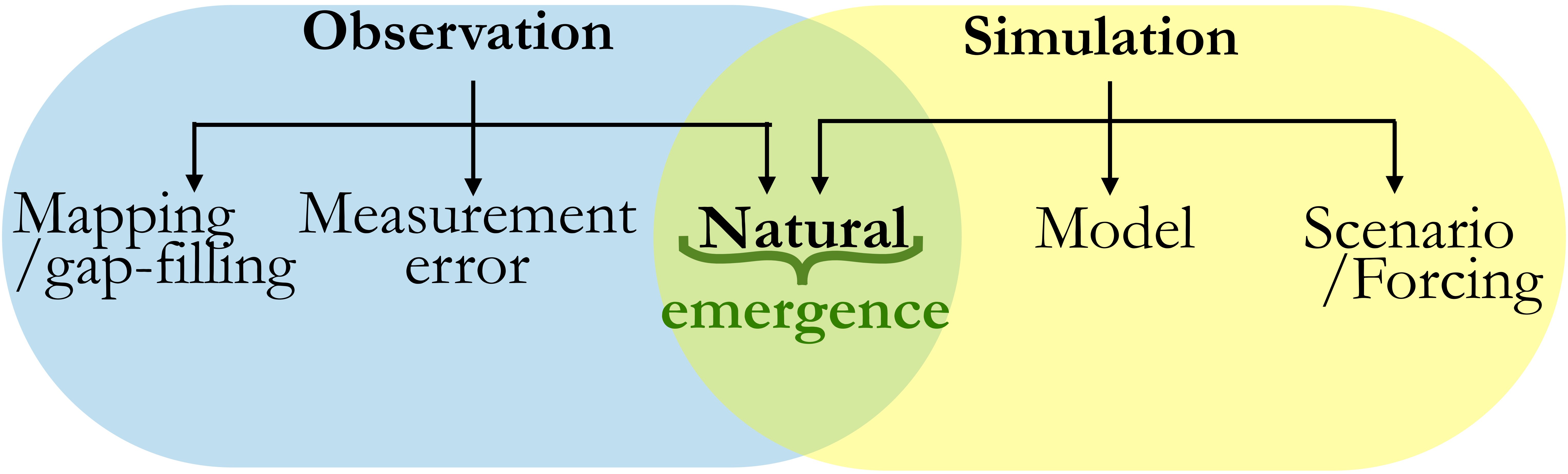

Figure from Schlunegger et al., 2019, in press

Time-of-Emergence

point in time the climate-change signal is statistically distinguishable from the noise

a multi-purpose metric

(1) inform observing system design

(2) inform impact timescales

(3) diagnostic which intelligently normalize anthropogenic responses across disparate variables

Sources of Uncertainty in Climate Observation and Simulation

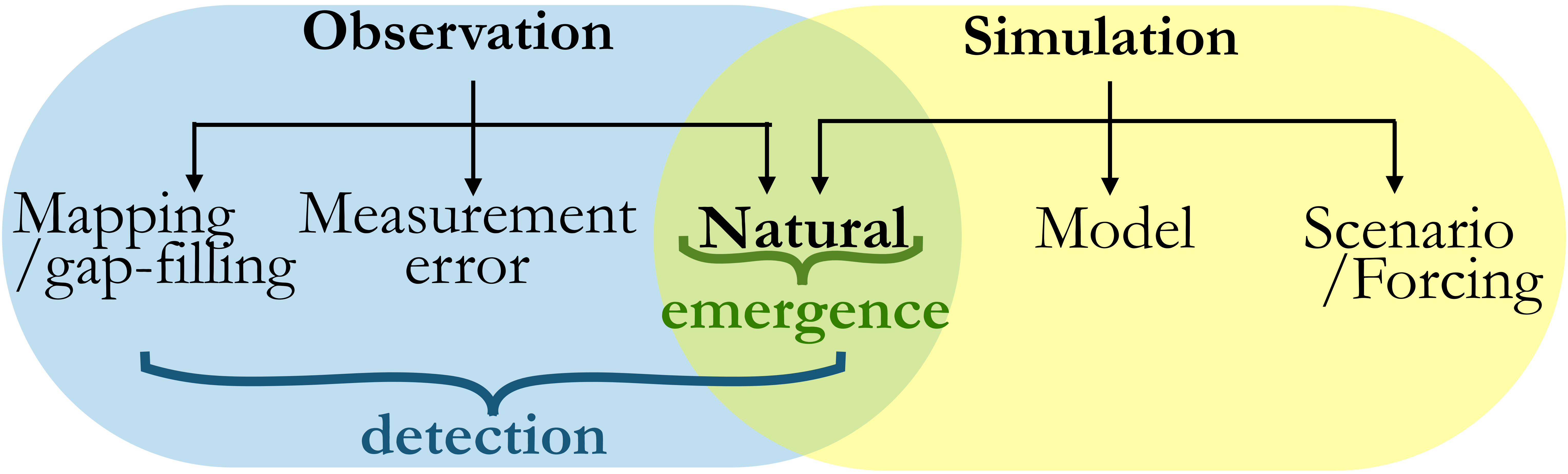

Figure from Schlunegger et al., 2019, in press

Time-of-Emergence

point in time the climate-change signal is statistically distinguishable from the noise

a multi-purpose metric

(1) inform observing system design

(2) inform impact timescales

(3) diagnostic which intelligently normalize anthropogenic responses across disparate variables

Sources of Uncertainty in Climate Observation and Simulation

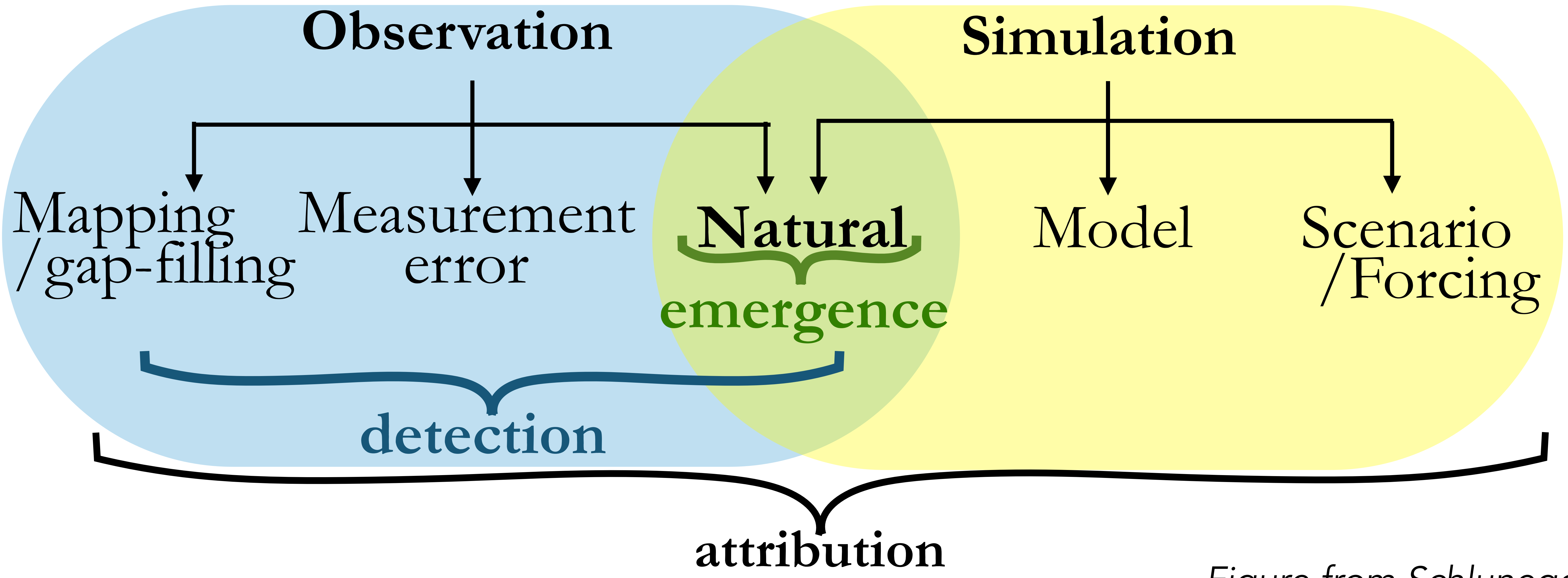

Figure from Schlunegger et al., 2019, in press

Time-of-Emergence

point in time the climate-change signal is statistically distinguishable from the noise

a multi-purpose metric

(1) inform observing system design

(2) inform impact timescales

(3) diagnostic which intelligently normalize anthropogenic responses across disparate variables

time at which trend exceeds the natural variability a system or organism is designed for or accustomed or adapted to

Time-of-Emergence

point in time the climate-change signal is statistically distinguishable from the noise

a multi-purpose metric

(1) inform observing system design

(2) inform impact timescales

(3) diagnostic which intelligently normalize anthropogenic responses across disparate variables

time at which trend exceeds the natural variability a system or organism is designed for or accustomed or adapted to

Time-of-Emergence

point in time the climate-change signal is statistically distinguishable from the noise

a multi-purpose metric

(1) inform observing system design

(2) inform impact timescales

(3) diagnostic which intelligently normalize anthropogenic responses across disparate variables

Time-of-Emergence Calculations

Signal = mean of 30 linear trends over given time period

Noise = standard deviation of 30 trends (~*normally distributed)*

SNR = Signal/Noise

Time-of-Emergence for anthropogenic trend is first year when **SNR > 2**. [95% Confidence]

Time-of-Emergence Calculations

Signal = mean of 30 linear trends over given time period

Noise = standard deviation of 30 trends (~*normally distributed)*

SNR = Signal/Noise

Time-of-Emergence for anthropogenic trend is first year when **SNR > 2**. [95% Confidence]

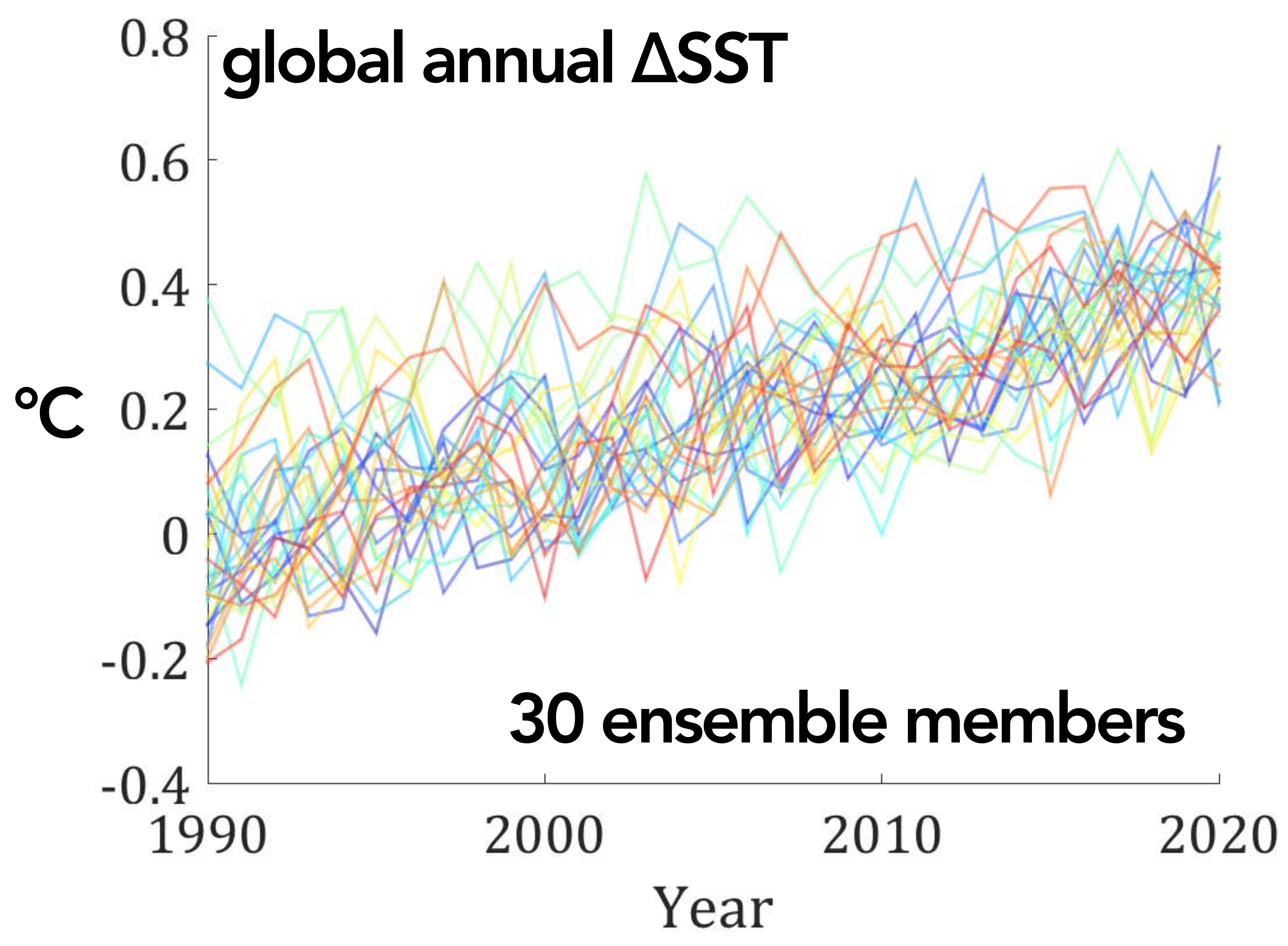

Time-of-Emergence Calculations

Signal = mean of 30 linear trends over given time period

Noise = standard deviation of 30 trends (~*normally distributed)*

SNR = Signal/Noise

Time-of-Emergence for anthropogenic trend is first year when **SNR > 2**. [95% Confidence]

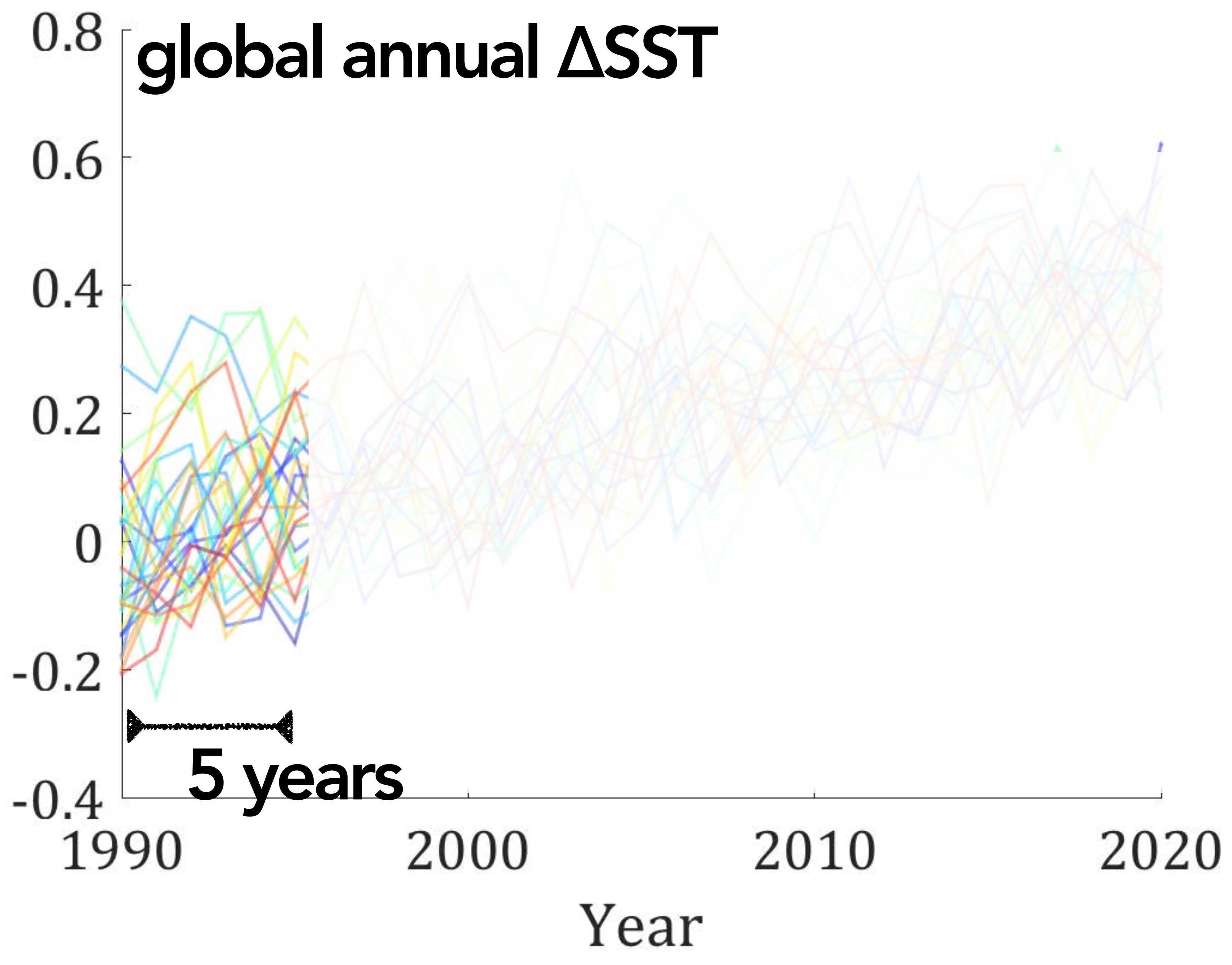

Time-of-Emergence Calculations

Signal = mean of 30 linear trends over given time period

Noise = standard deviation of 30 trends (~*normally distributed)*

SNR = Signal/Noise

Time-of-Emergence for anthropogenic trend is first year when **SNR > 2**. [95% Confidence]

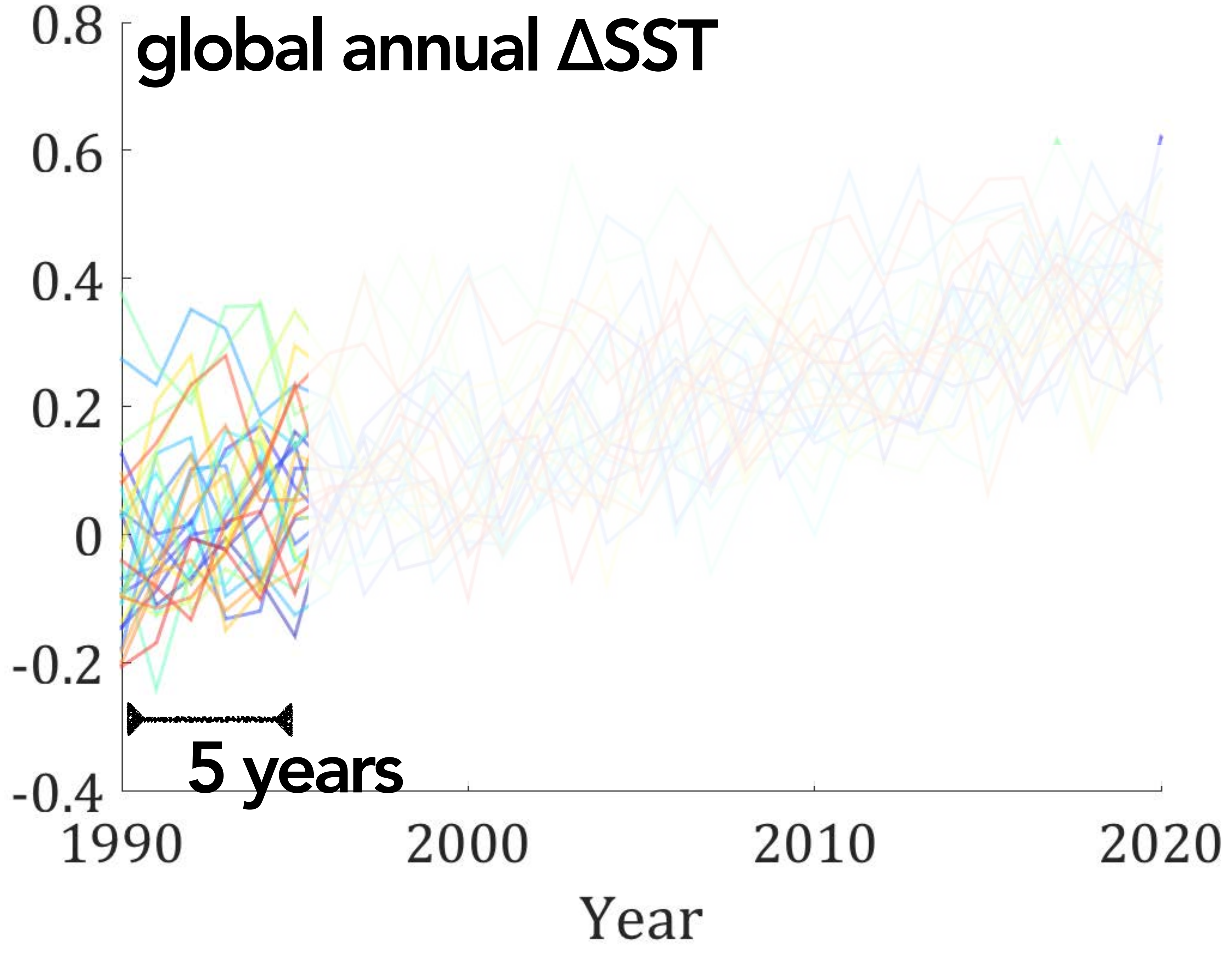

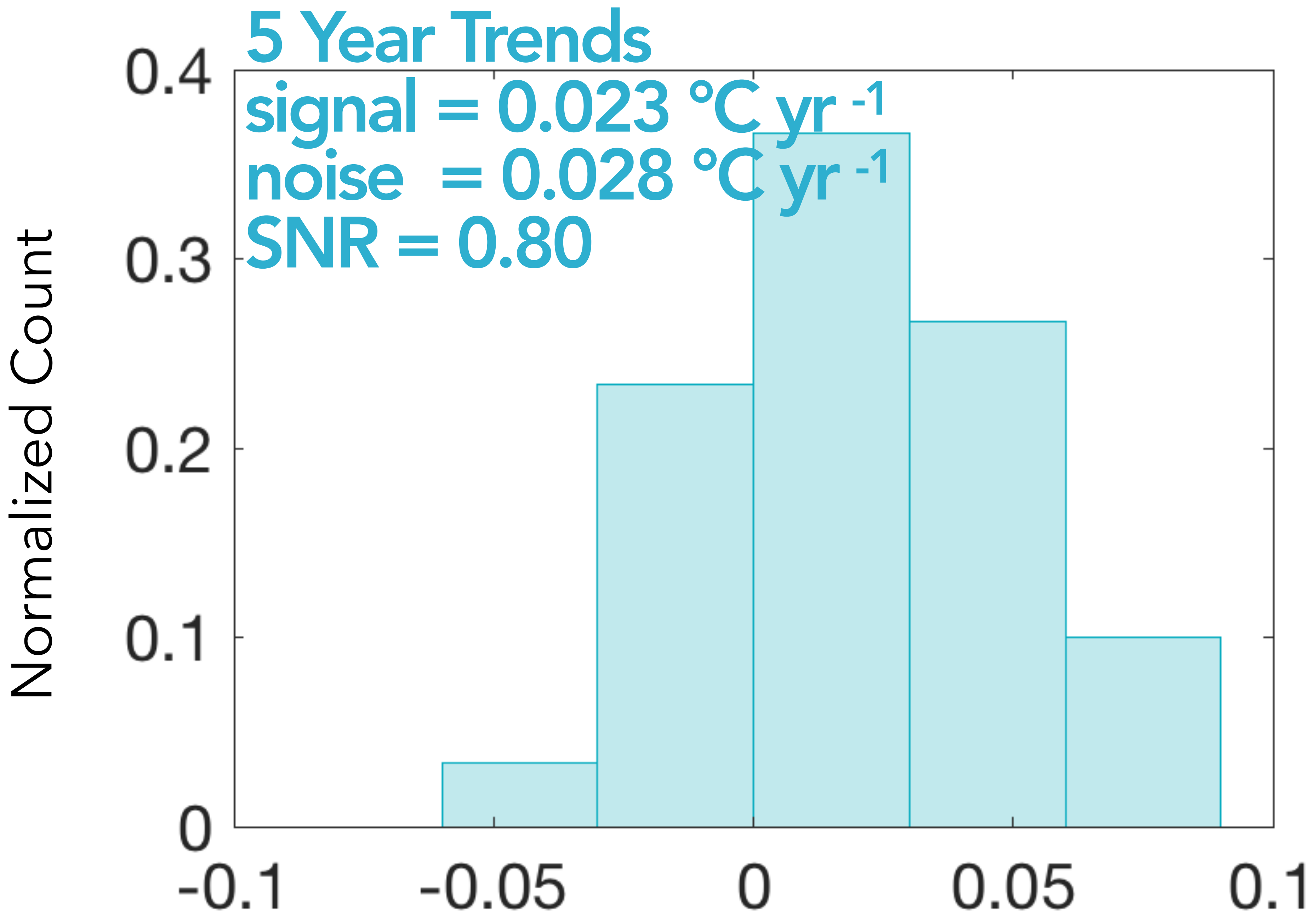

Time-of-Emergence Calculations

Signal = mean of 30 linear trends over given time period

Noise = standard deviation of 30 trends (~*normally distributed)*

SNR = Signal/Noise

Time-of-Emergence for anthropogenic trend is first year when **SNR > 2**. [95% Confidence]

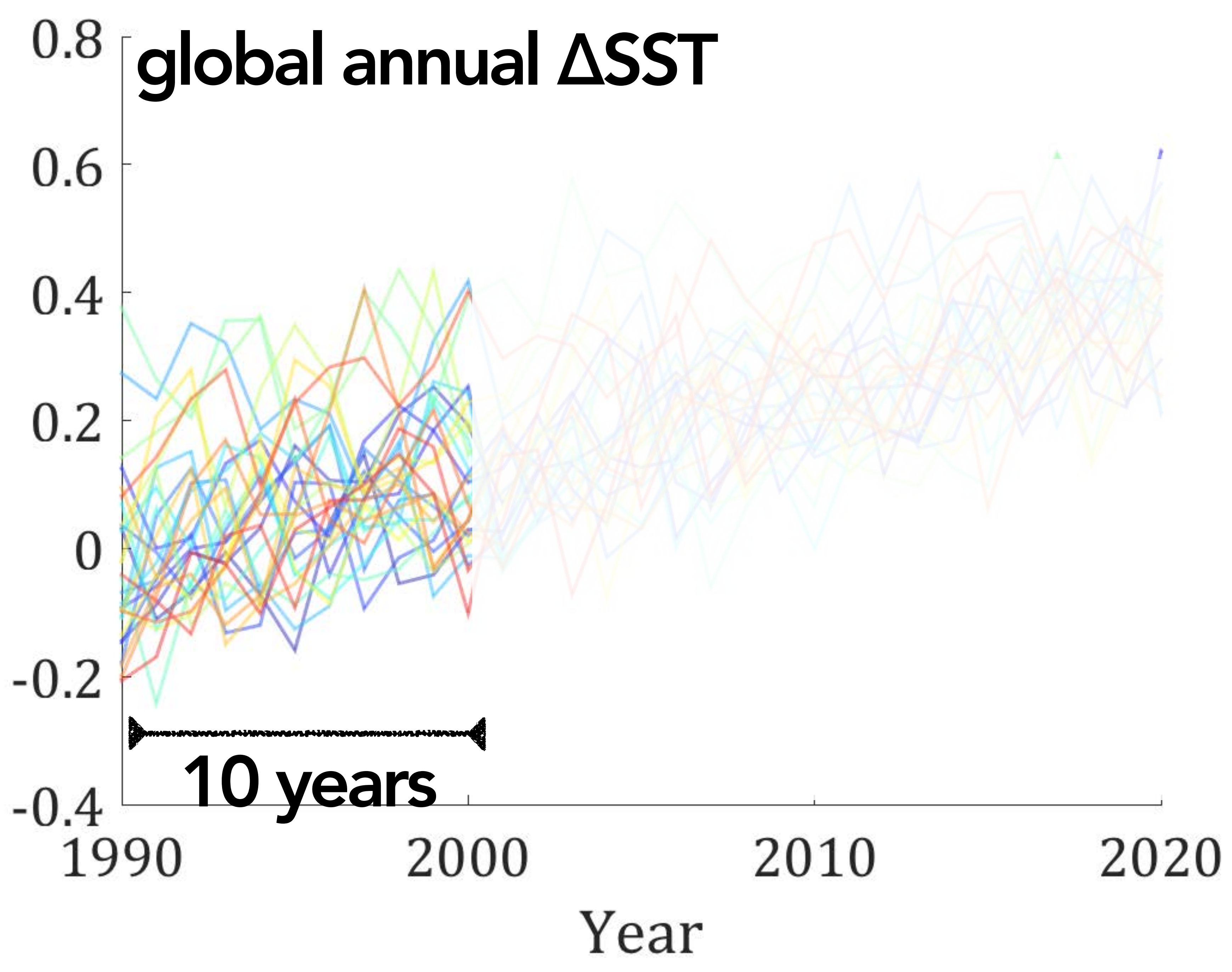

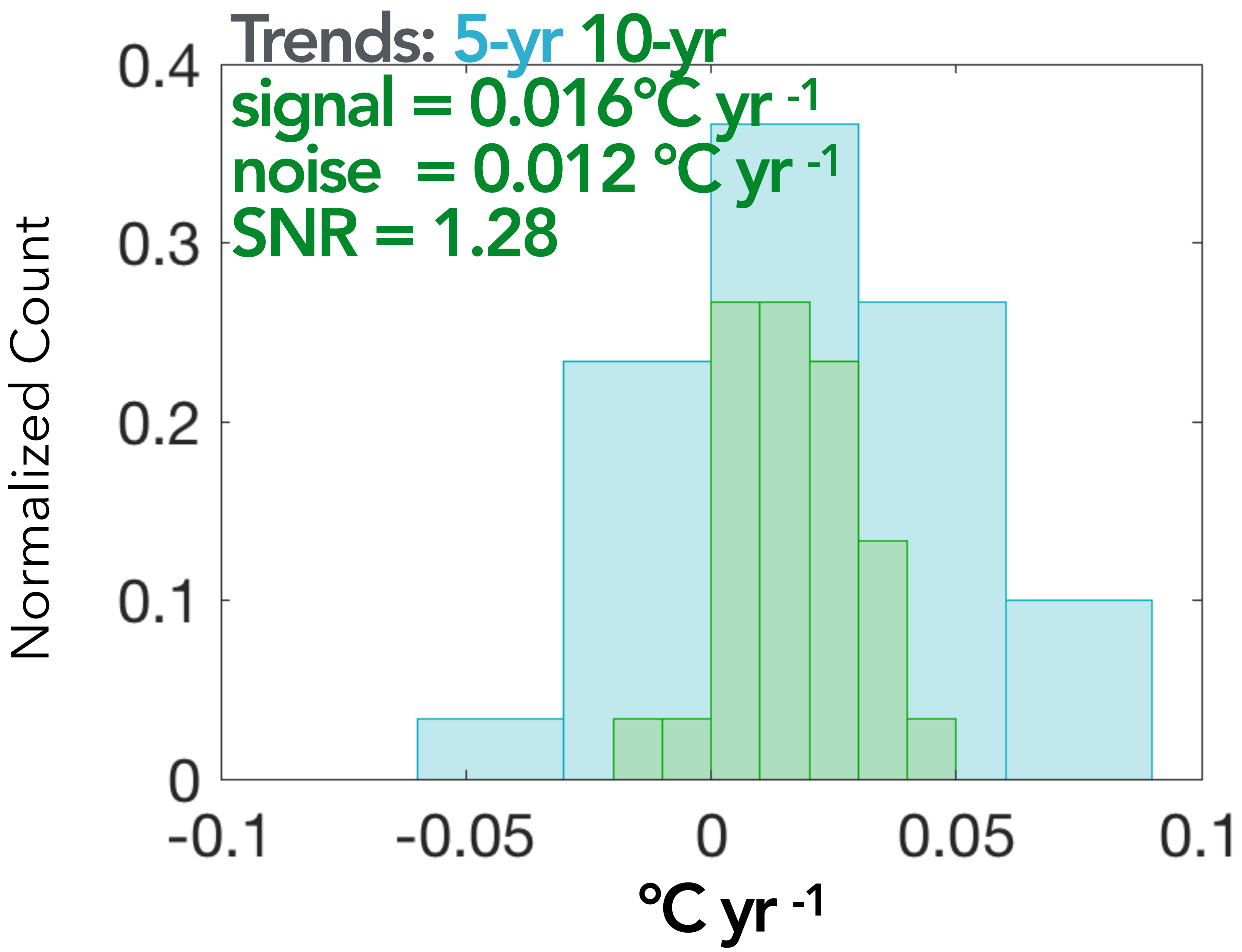

Time-of-Emergence Calculations

Signal = mean of 30 linear trends over given time period

Noise = standard deviation of 30 trends (~*normally distributed)*

SNR = Signal/Noise

Time-of-Emergence for anthropogenic trend is first year when **SNR > 2**. [95% Confidence]

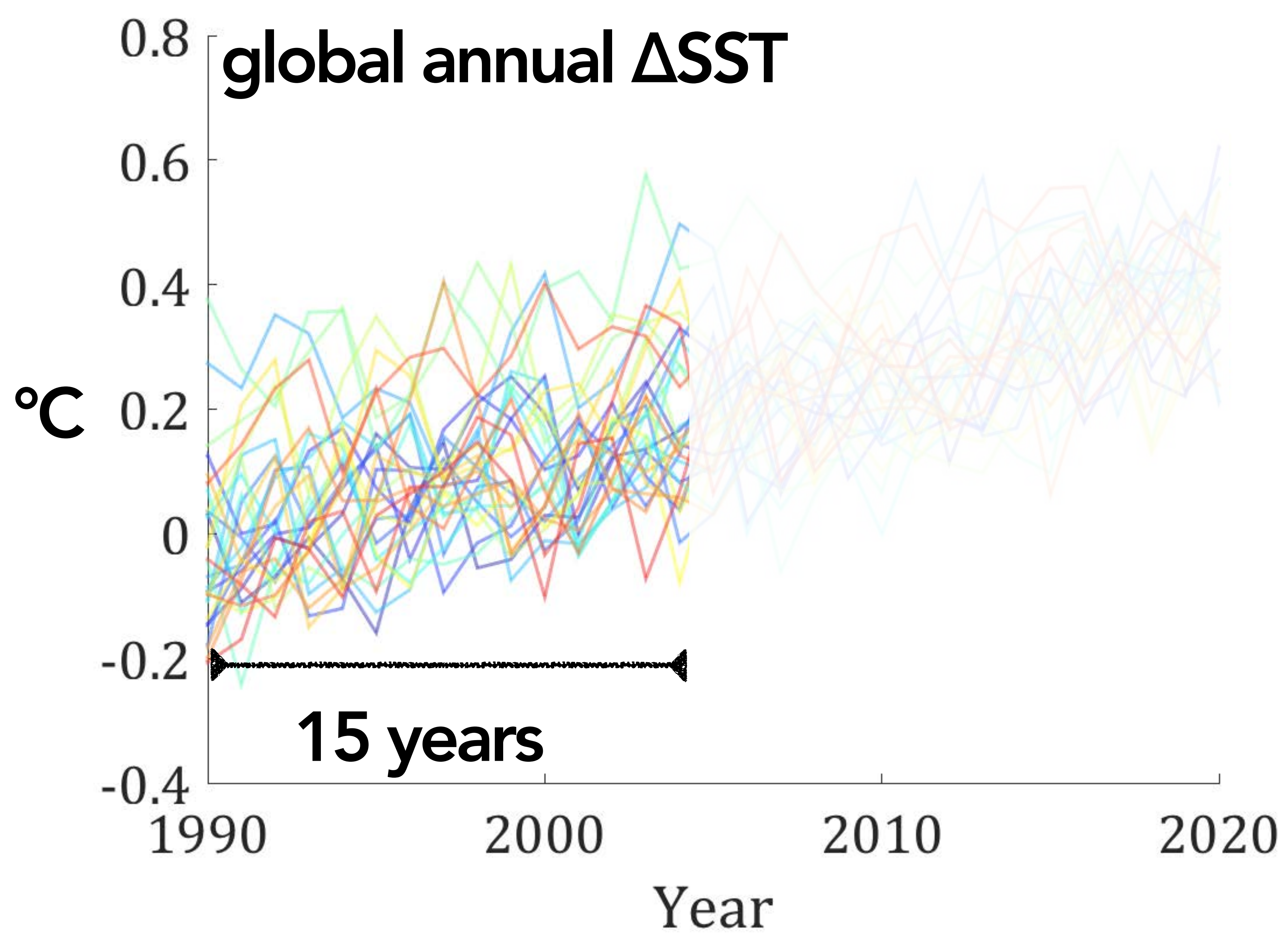

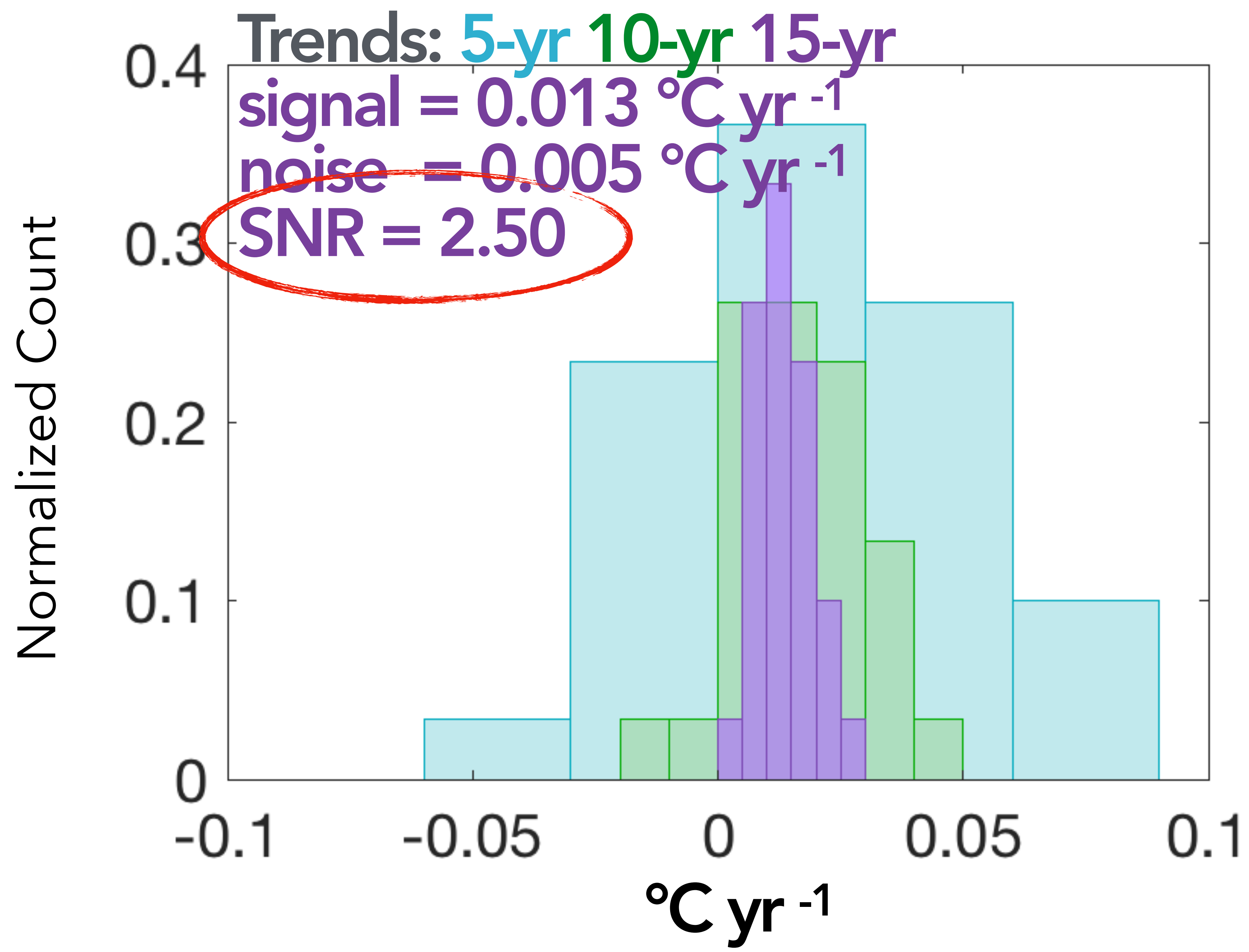

Time-of-Emergence Calculations

Signal = mean of 30 linear trends over given time period

Noise = standard deviation of 30 trends (~*normally distributed)*

SNR = Signal/Noise

Time-of-Emergence for anthropogenic trend is first year when **SNR > 2**. [95% Confidence]

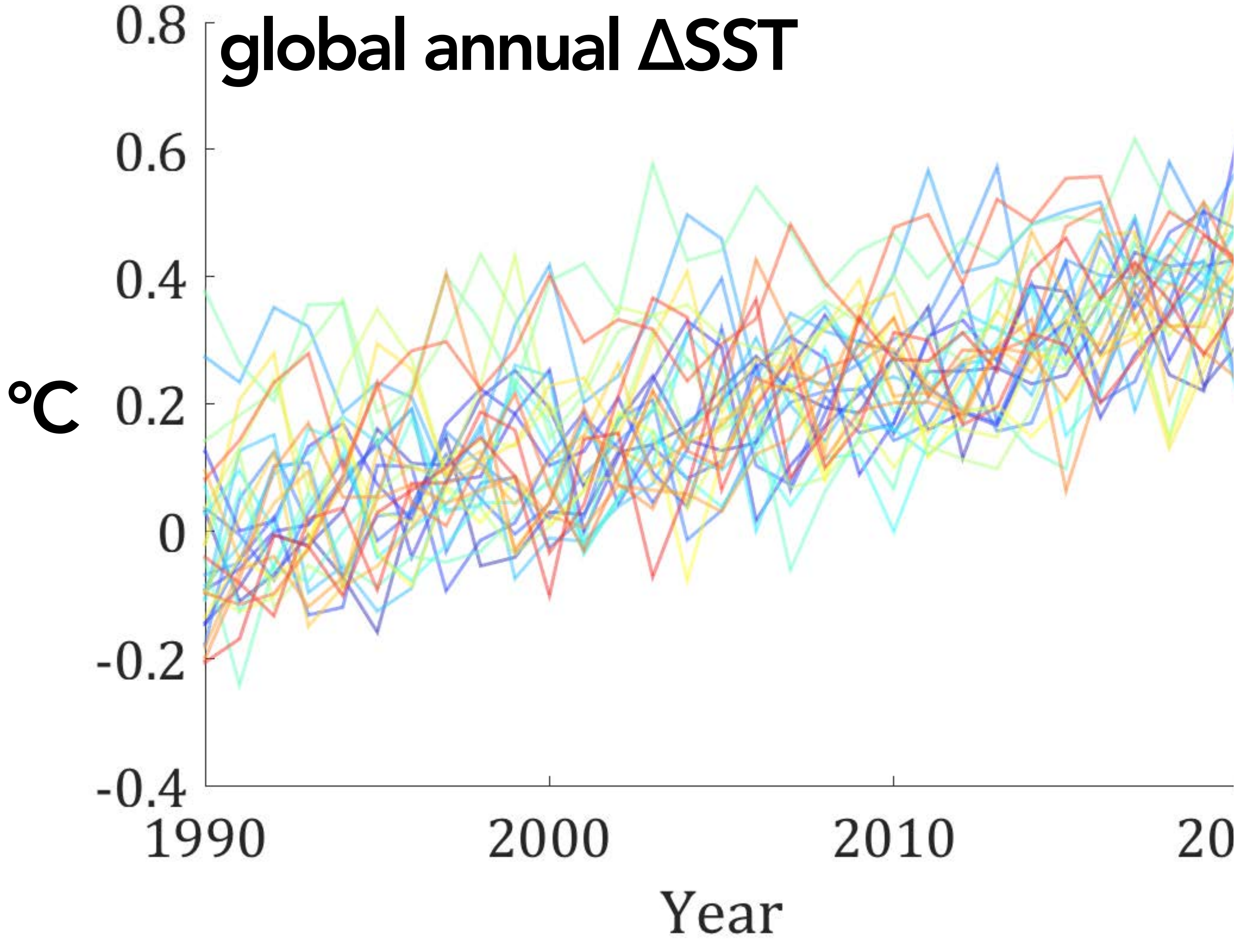

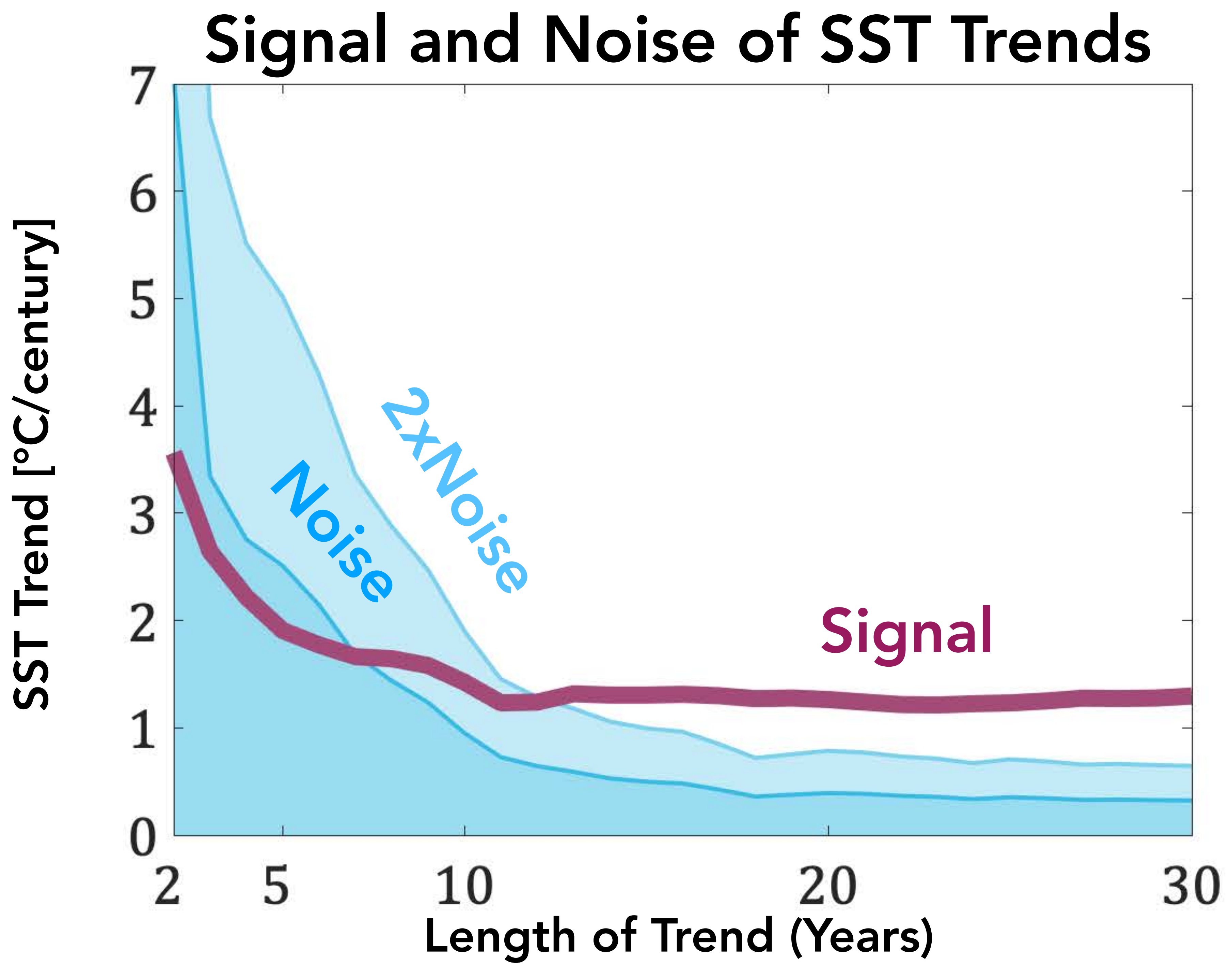

Time-of-Emergence Calculations

Signal = mean of 30 linear trends over given time period

Noise = standard deviation of 30 trends (~*normally distributed)*

SNR = Signal/Noise

Time-of-Emergence for anthropogenic trend is first year when **SNR > 2**. [95% Confidence]

GLOBAL

Time-of-Emergence Calculations

Signal = mean of 30 linear trends over given time period

Noise = standard deviation of 30 trends (~*normally distributed)*

SNR = Signal/Noise

Time-of-Emergence for anthropogenic trend is first year when **SNR > 2**. [95% Confidence]

GLOBAL

REGIONAL

Time-of-Emergence Calculations

Signal = mean of 30 linear trends over given time period

Noise = standard deviation of 30 trends (~*normally distributed)*

SNR = Signal/Noise

Time-of-Emergence for anthropogenic trend is first year when **SNR > 2**. [95% Confidence]

GLOBAL

REGIONAL

LOCAL / GRID-CELL

Large Ensemble Experiments from 4 Earth System Models

using business as usual (RCP8.5)
and moderate mitigation (RCP4.5) scenarios

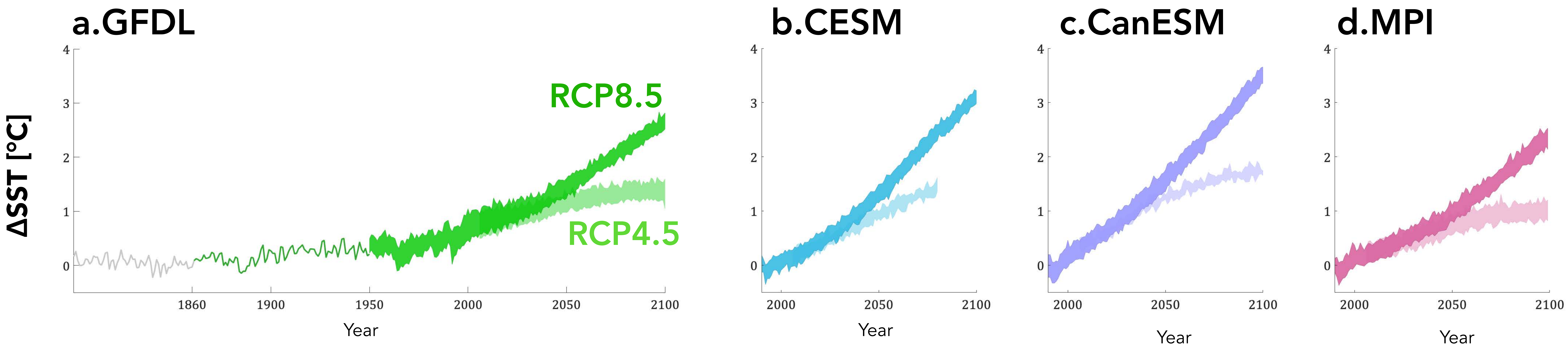

Large Ensemble Experiments from 4 Earth System Models

using business as usual (RCP8.5)
and moderate mitigation (RCP4.5) scenarios

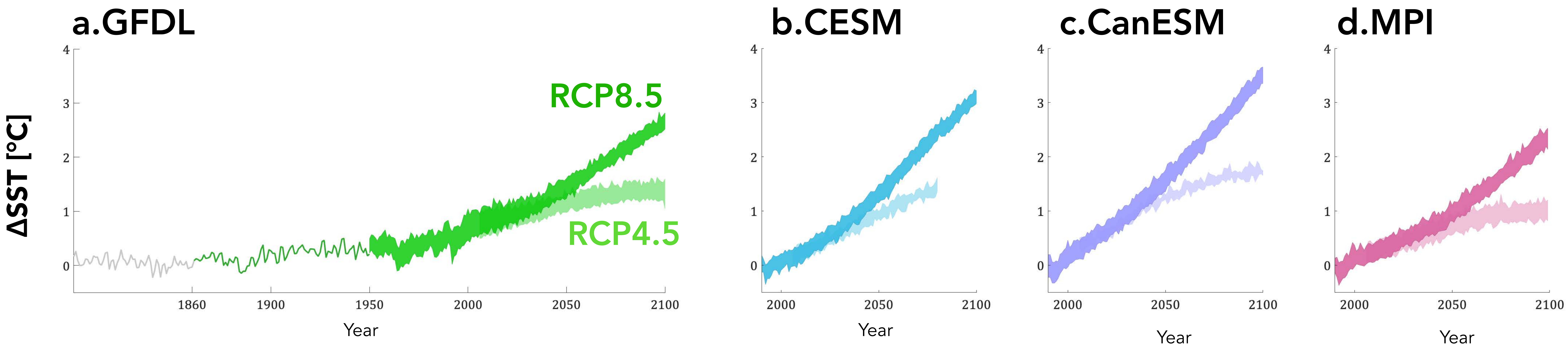

can test the model- and scenario-sensitivity of emergence times

Large Ensemble Experiments from 4 Earth System Models

Changes in key ocean observables over the 21st century

GFDL-ESM2M CESM1 CanESM2 MPI ESM LR

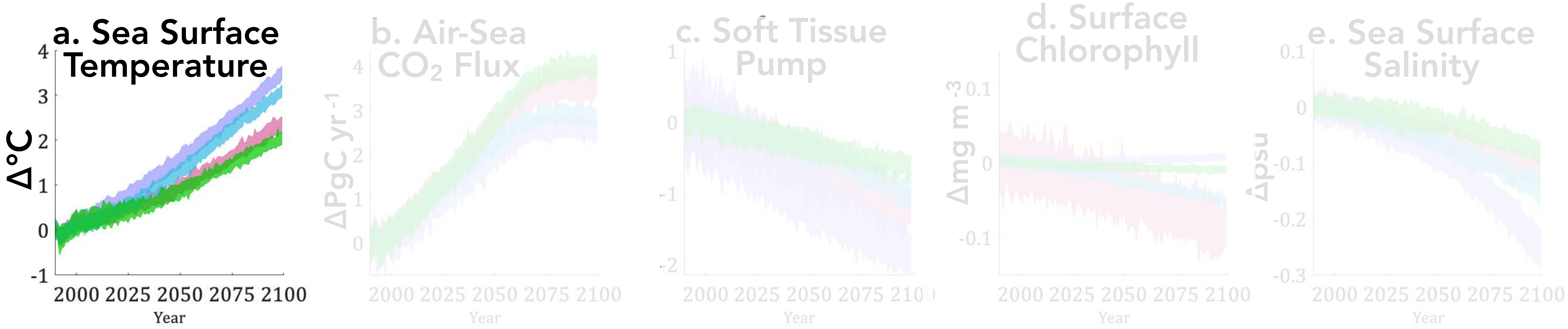

3-5°C Warming by 2100

Large Ensemble Experiments from 4 Earth System Models

Changes in key ocean observables over the 21st century

GFDL-ESM2M CESM1 CanESM2 MPI ESM LR

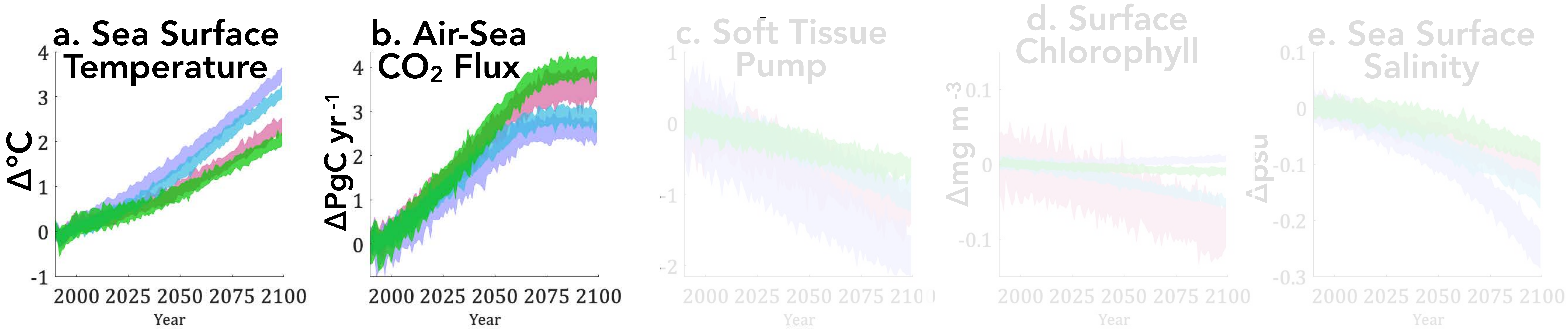

3-5°C Warming by 2100

Inverse relationship between ΔT and CO_2 uptake

Large Ensemble Experiments from 4 Earth System Models

Changes in key ocean observables over the 21st century

GFDL-ESM2M CESM1 CanESM2 MPI ESM LR

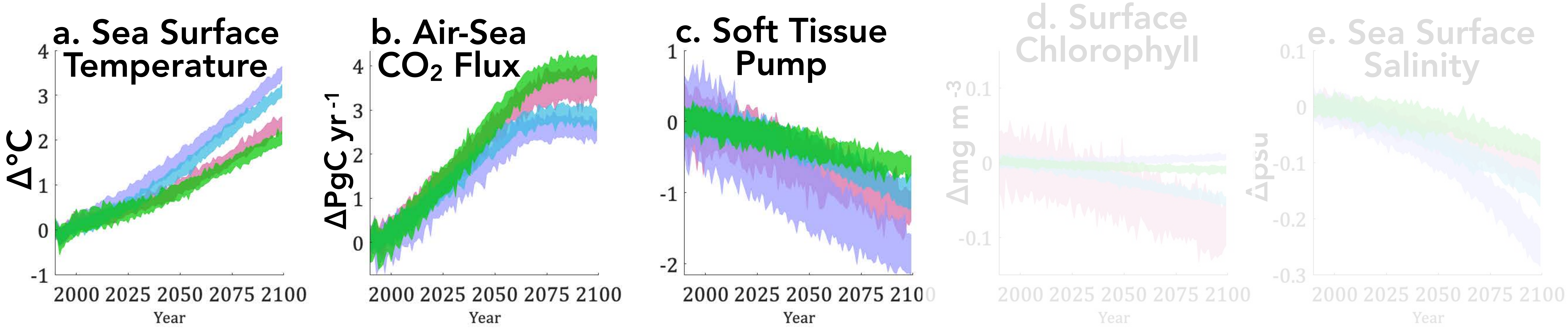

3-5°C Warming by 2100

Inverse relationship between ΔT and CO_2 uptake

All models reduced bio export, magnitude uncertain

Large Ensemble Experiments from 4 Earth System Models

Changes in key ocean observables over the 21st century

GFDL-ESM2M CESM1 CanESM2 MPI ESM LR

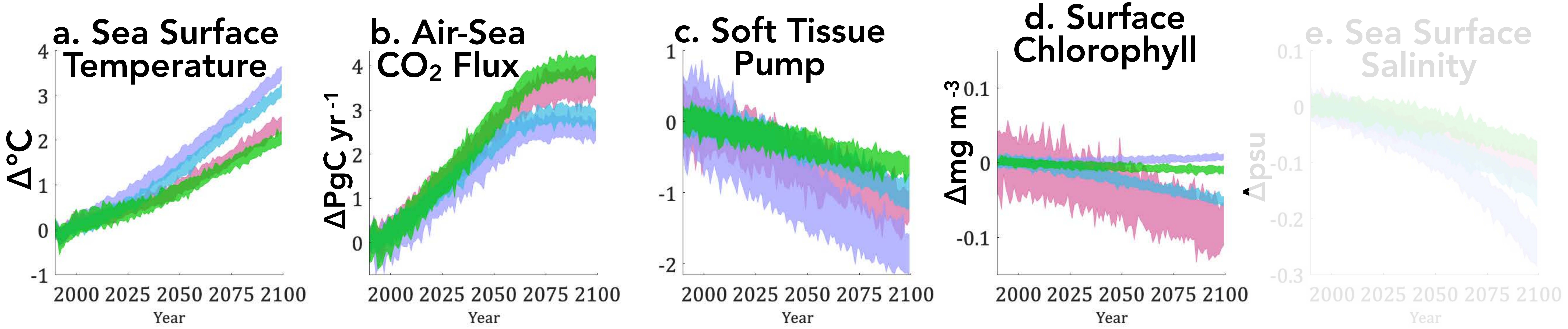

3-5°C Warming by 2100

Inverse relationship between ΔT and CO_2 uptake

All models reduced bio export, magnitude uncertain

Neutral or declining chlorophyll

Large Ensemble Experiments from 4 Earth System Models

Changes in key ocean observables over the 21st century

GFDL-ESM2M CESM1 CanESM2 MPI ESM LR

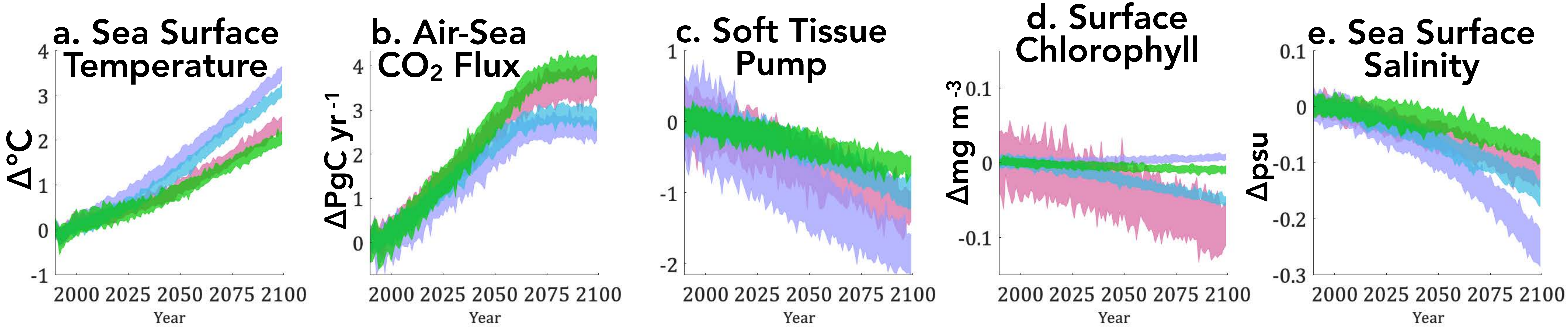

3-5°C Warming by 2100

Inverse relationship between ΔT and CO_2 uptake

All models reduced bio export, magnitude uncertain

Neutral or declining chlorophyll

Global freshening, magnitude uncertain

Time of Emergence for Global and Regional Trends

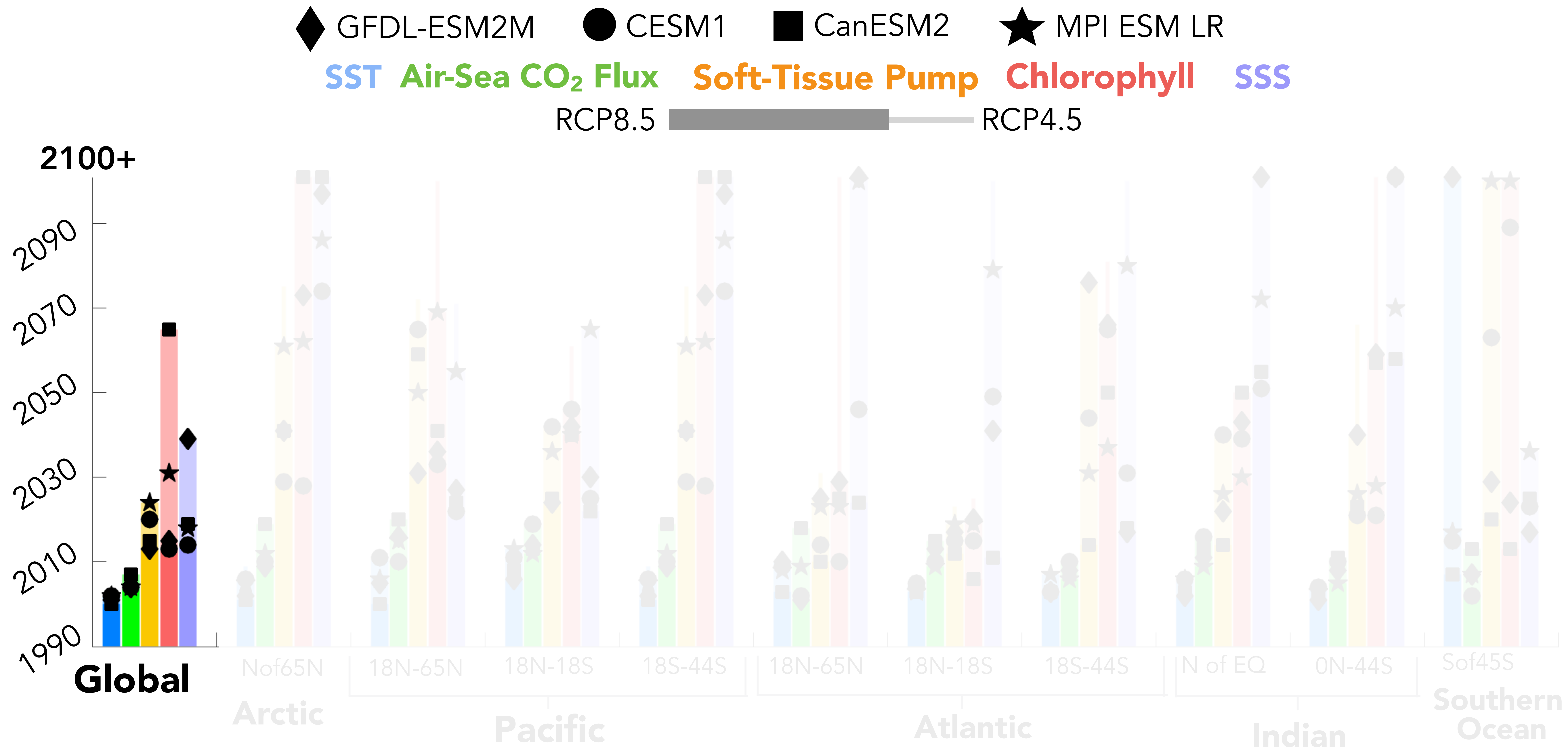

LEs agree global SST and Air-Sea CO_2 flux emergent within <2 decades

Longer ToEs and less LE-agreement for the biological variables and SSS

Time of Emergence for Global and Regional Trends

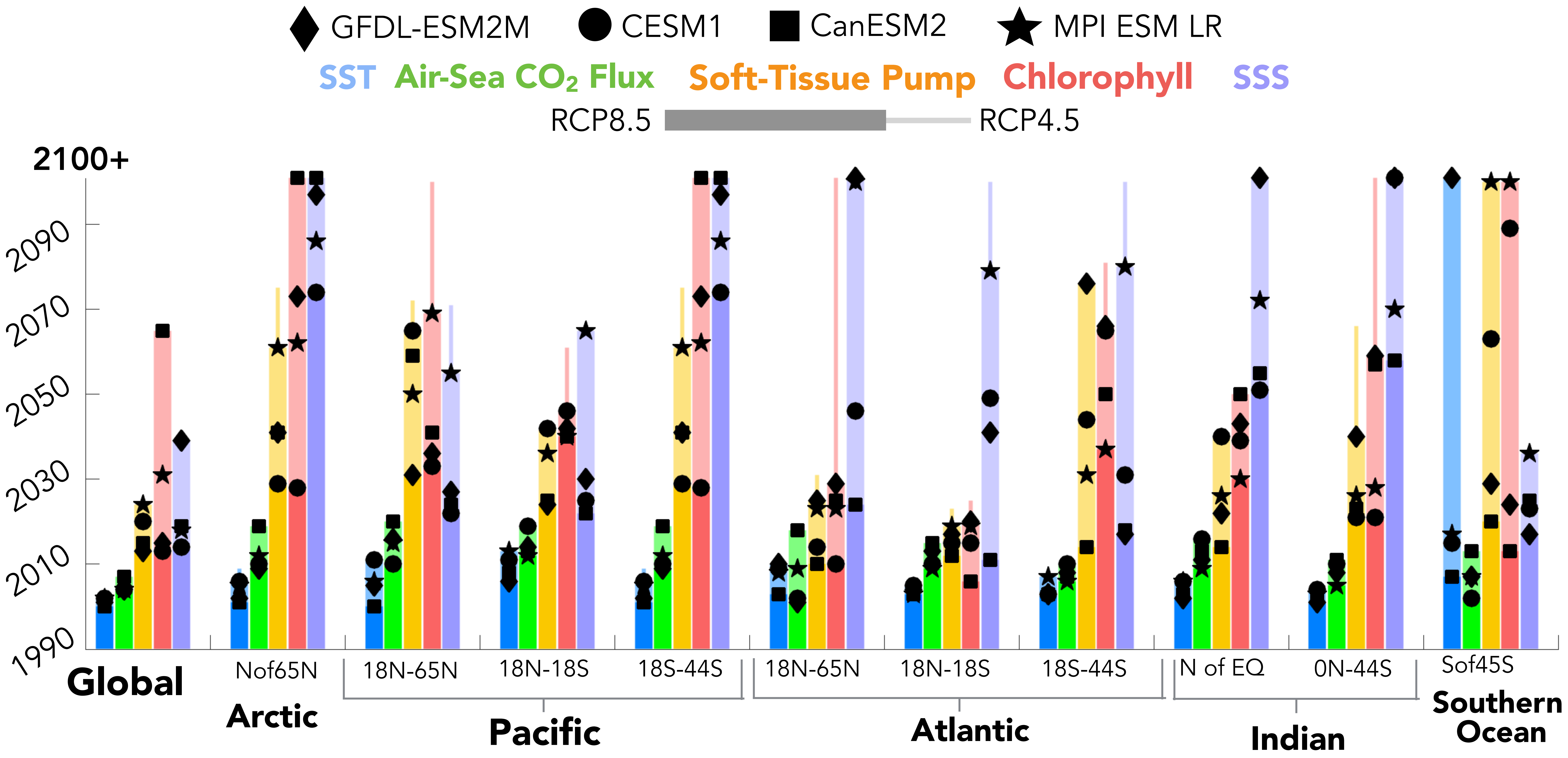

LEs agree regional SST and Air-Sea CO_2 flux emergent within <3 decades

Longer ToEs and less LE-agreement for the biological variables and SSS

Time of Emergence for Global and Regional Trends

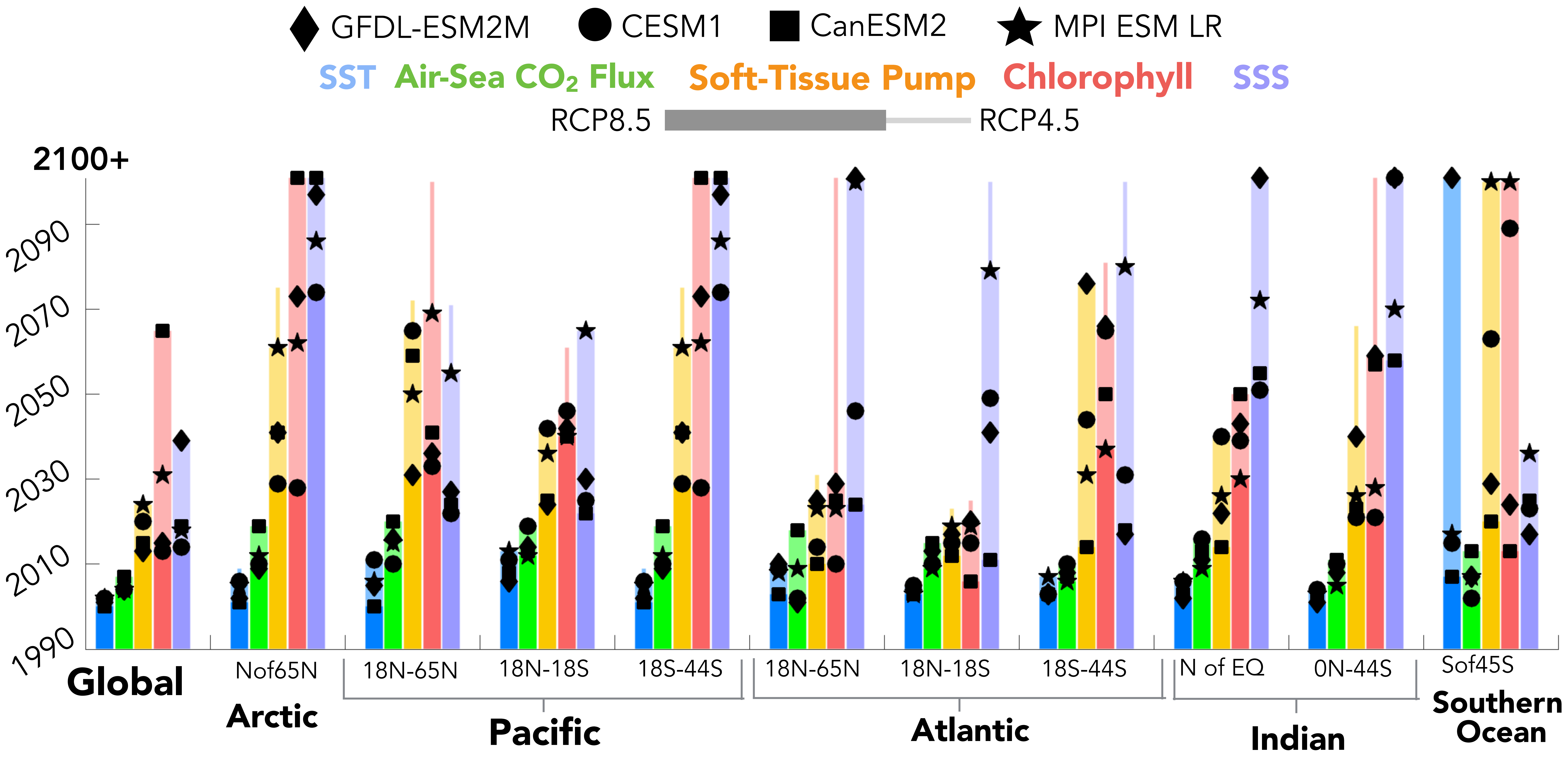

For some regions, mitigation can delay or deter emergence of biological impacts and second order physical changes, like changes in SSS.

Time of Emergence for Local Trends

Mean of the 4 LEs, white hatching over areas of model-disagreement

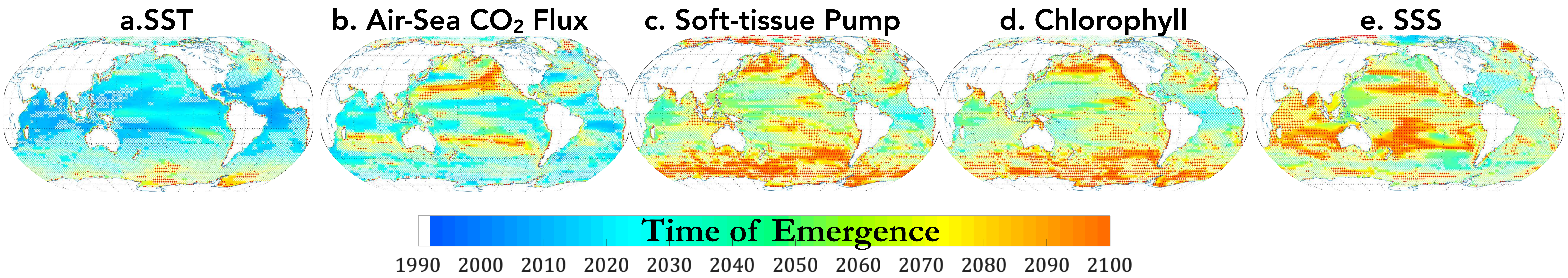

Time of Emergence for Local Trends

Mean of the 4 LEs, white hatching over areas of model-disagreement

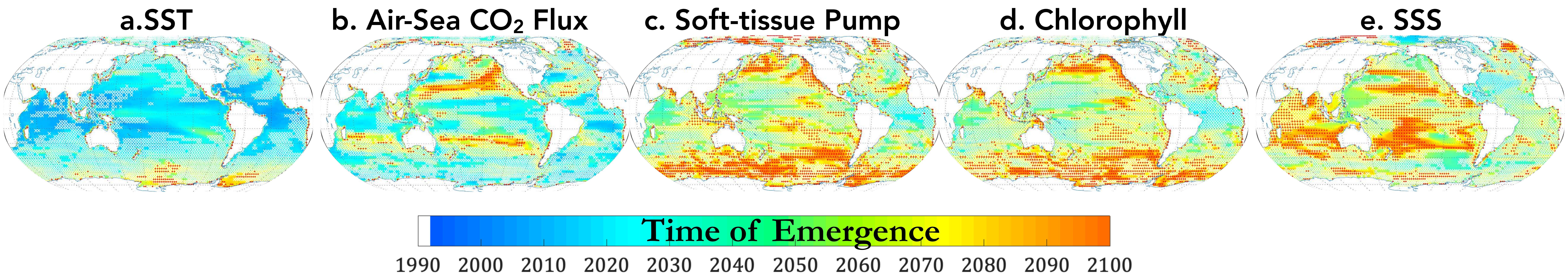

LEs agree on early emergence of SST over tropics and extra-tropics

LEs agree on non-emergence CO_2 fluxes over subtropics

Long but inconsistent ToEs for soft-tissue pump, chlorophyll and SSS

Partitioning Uncertainty (e.g. Hawkins and Sutton) using multiple Large Ensembles

GLOBAL DOMAIN

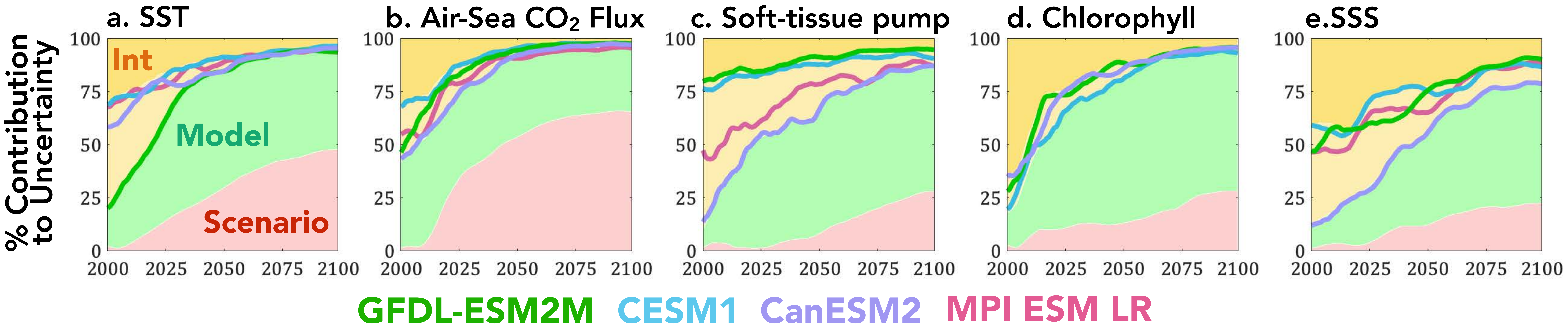

Partitioning Uncertainty (e.g. Hawkins and Sutton) using multiple Large Ensembles

GLOBAL DOMAIN

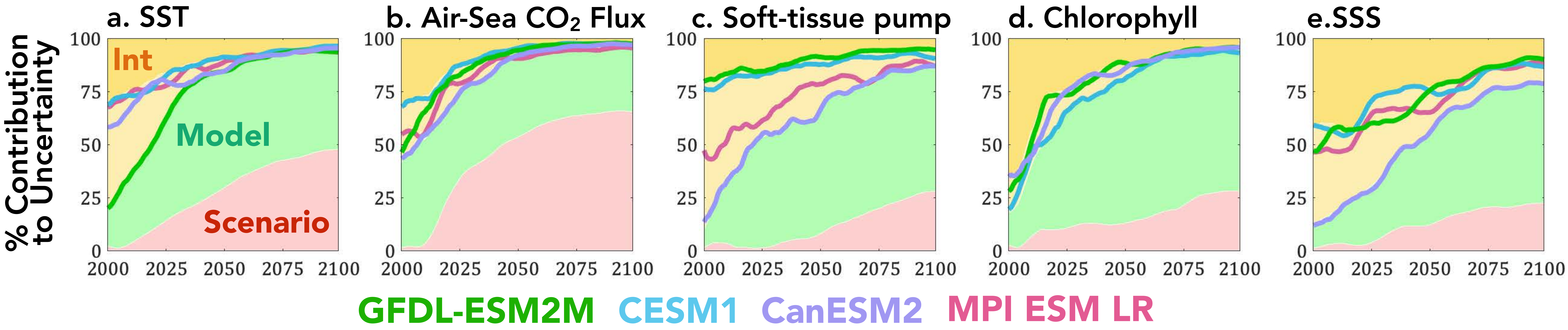

Model uncertainty important for all variables

Internal variability estimates ***can*** differ significantly between the ESMs

Partitioning Uncertainty (e.g. Hawkins and Sutton) using multiple Large Ensembles

GLOBAL DOMAIN

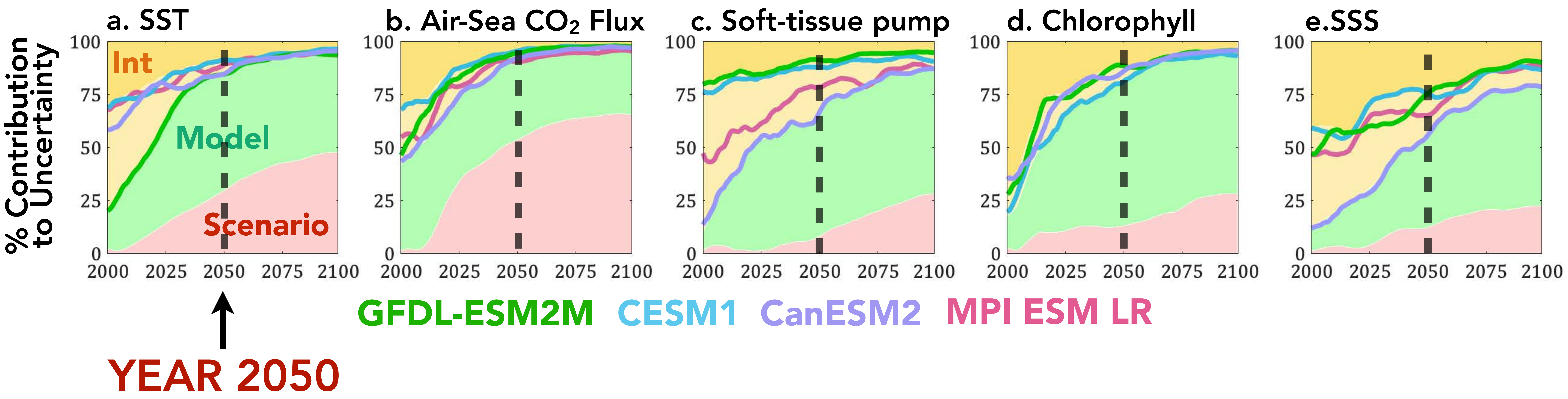

Partitioning Uncertainty (e.g. Hawkins and Sutton) using multiple Large Ensembles

AT YEAR 2050

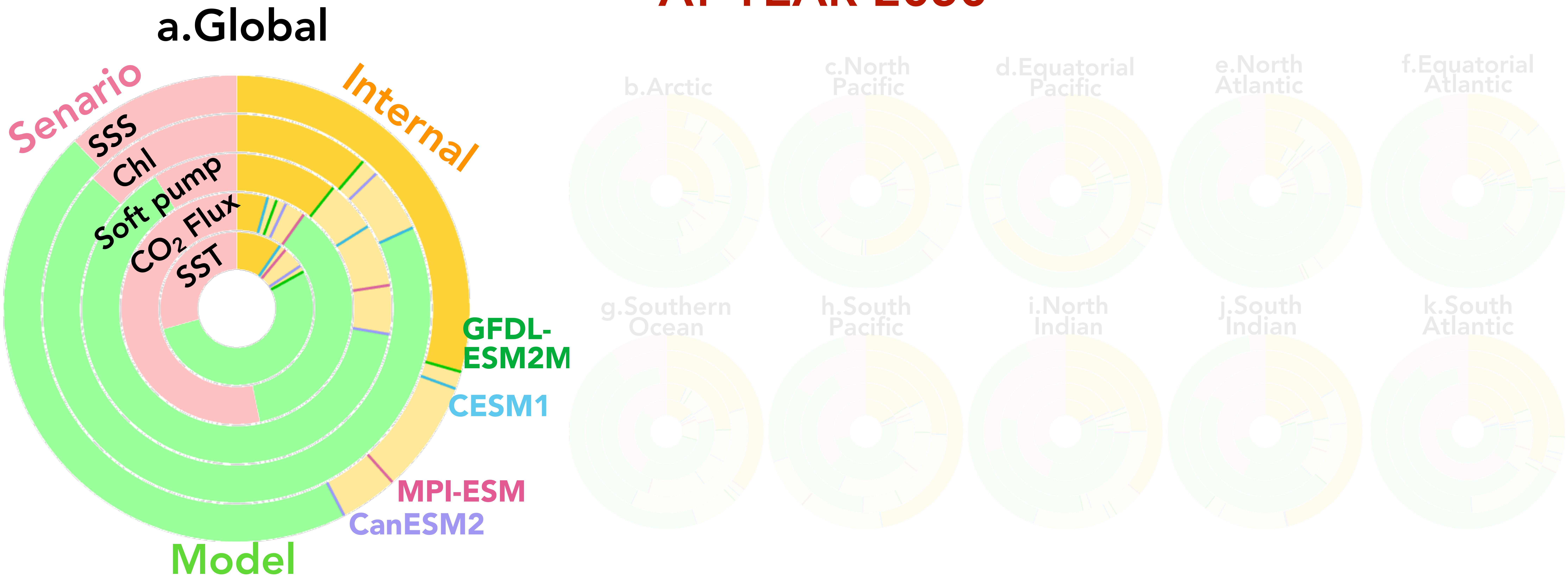

Partitioning Uncertainty (e.g. Hawkins and Sutton) using multiple Large Ensembles

AT YEAR 2050

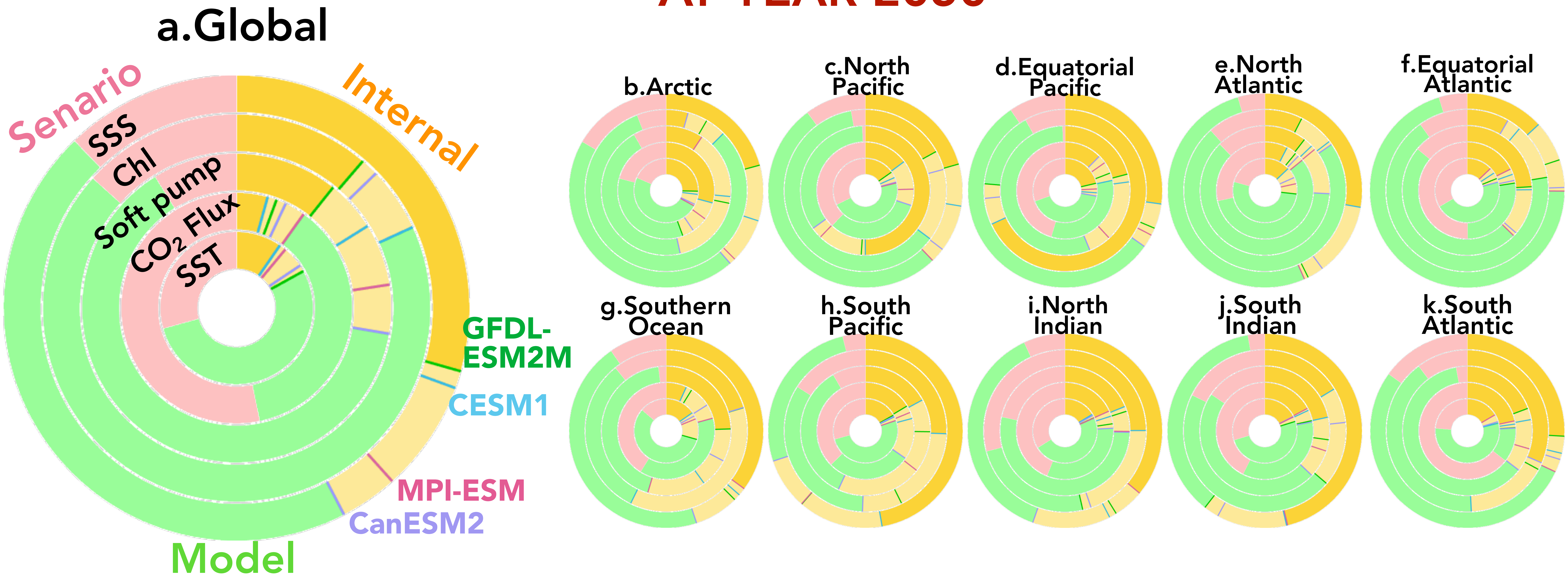

Partitioning Uncertainty (e.g. Hawkins and Sutton) using multiple Large Ensembles

AT YEAR 2050

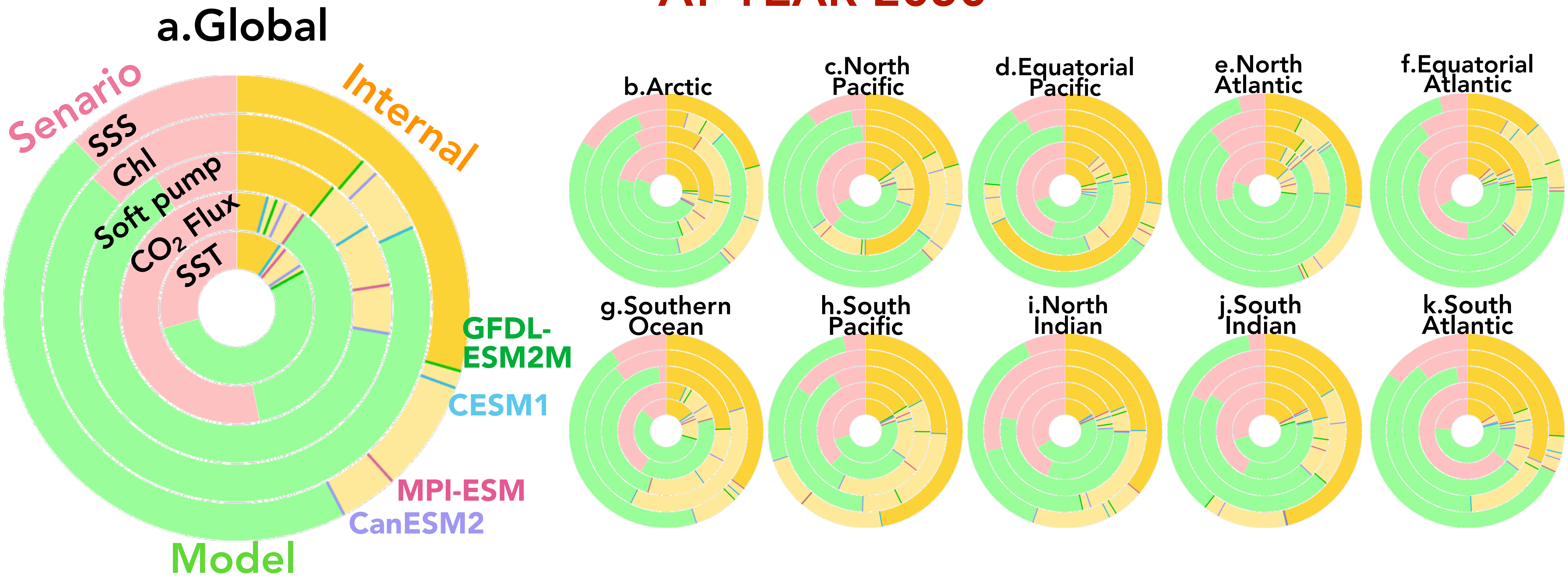

Internal variability estimates important at regional scales,

and can differ significantly between ESMs, for bio-parameters and SSS

Results

Time of Emergence

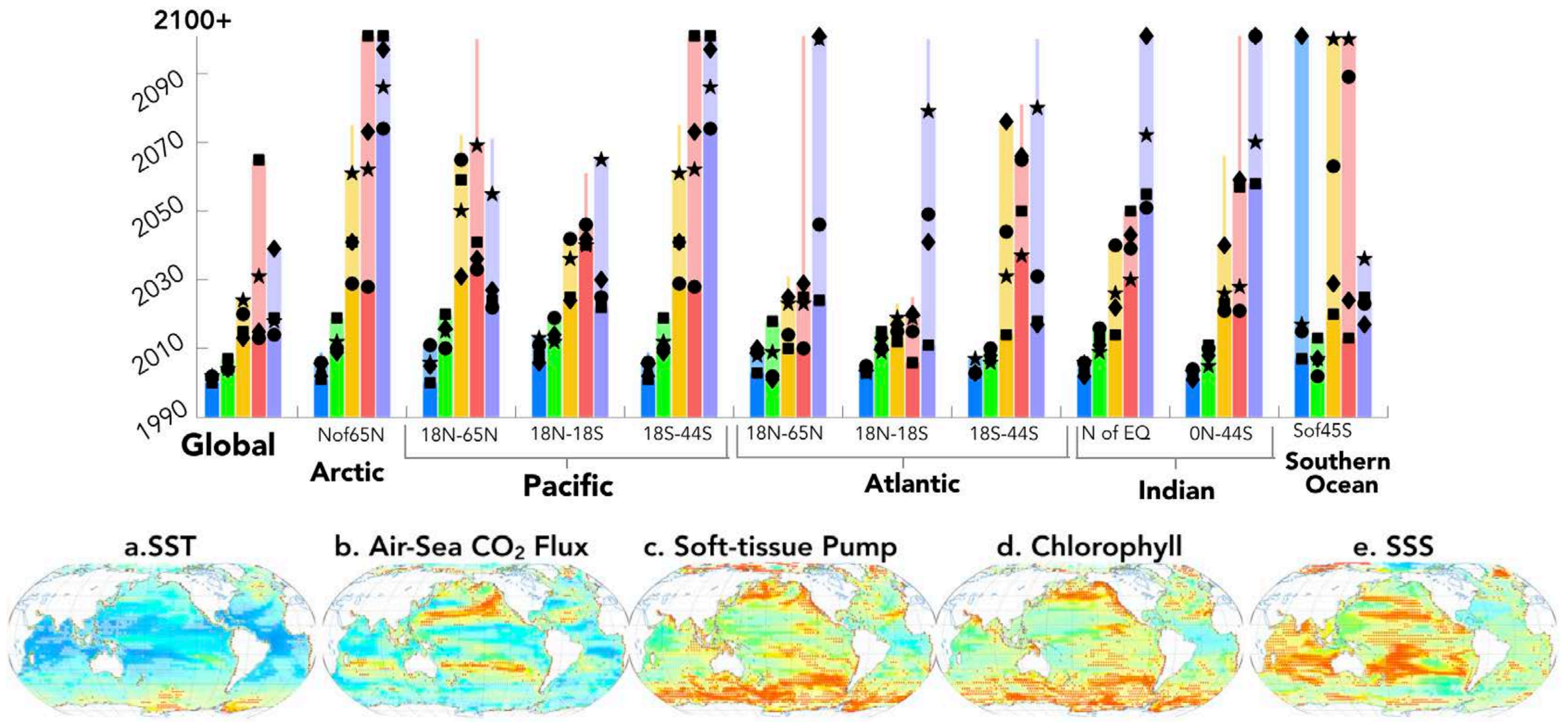

Partitioning Uncertainty

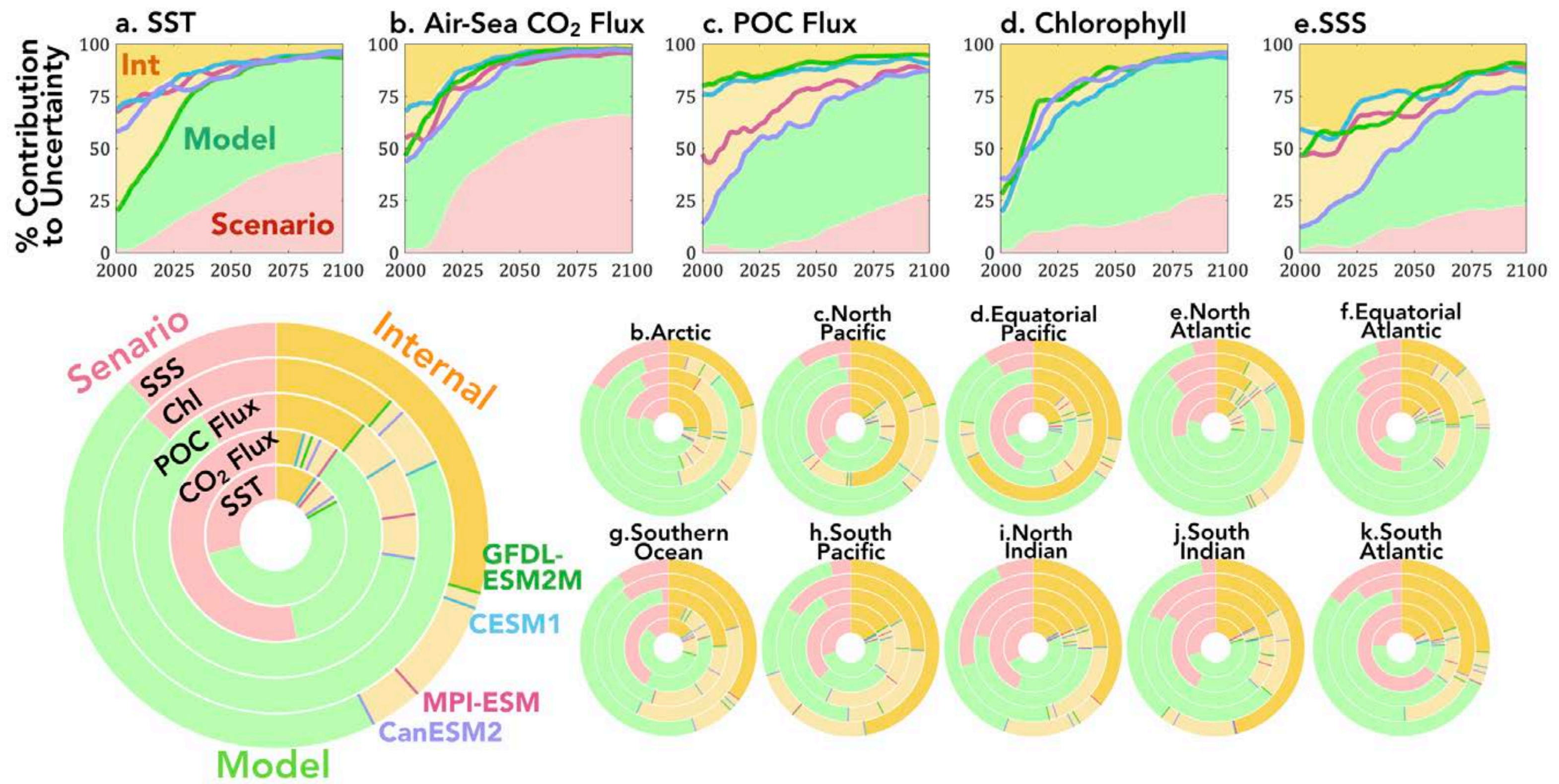

Take Aways

- ToE's in the ocean ranging from under a decade to over a century
- Time-lag of drivers: rapid interaction with atm CO_2 & heat, slow circulation adjust
- Consistent chronology amongst representative suite of ESMs
- LE's reveal internal variability can differ significantly between ESMs, but structural uncertainty generally dominate
- **>> GFDL LE output available @ http://poseidon.princeton.edu**

Partitioning Projection Uncertainty in 4 ESM LEs

$$U_M(t) = Max\{\bar{LE}_{m,85}(t, m = 1:4)\} - Min\{\bar{LE}_{m,85}(t, m = 1:4)\} \quad (1)$$

Where t is the years between 1990 and 2100 and m denotes the 4 ESMs. We use the RCP8.5 LEs for two reasons: (1) this is the scenario with the most ensemble members available, at least 30 members for each ESM and (2) the larger forcing that persists through the century will reveal model differences more effectively than will the moderate or declining forcing scenario.

We estimate U_S by averaging across both ensemble members and ESMs,

$$U_S(t) = Mean\{\bar{LE}_{85}(t, m = 1:4)\} - Mean\{\bar{LE}_{45}(t, m = 1:4)\} \quad (2)$$

where t is the years between 2006 and 2100 and m denotes the 4 ESMs.

$$U_{IV}(m, t) = Max\{LE_{m,85}(t, e = 1:30)\} - Min\{LE_{m,85}(t, e = 1:30)\} \quad (3)$$

where t is the years between 1990 and 2100, m denotes the 4 ESMs, and e denotes the ensemble members in each LE. We use the RCP8.5 LEs as this is the scenario with the most ensemble members available for each of the LEs.

Sequence of Emerging Anthropogenic Signals in the Ocean

Reduced Emergence timescales with optimized sampling strategies

Sequence of Emerging Anthropogenic Signals in the Ocean

Pumps (in bold) and ocean tracers and process to which the pumps are coupled

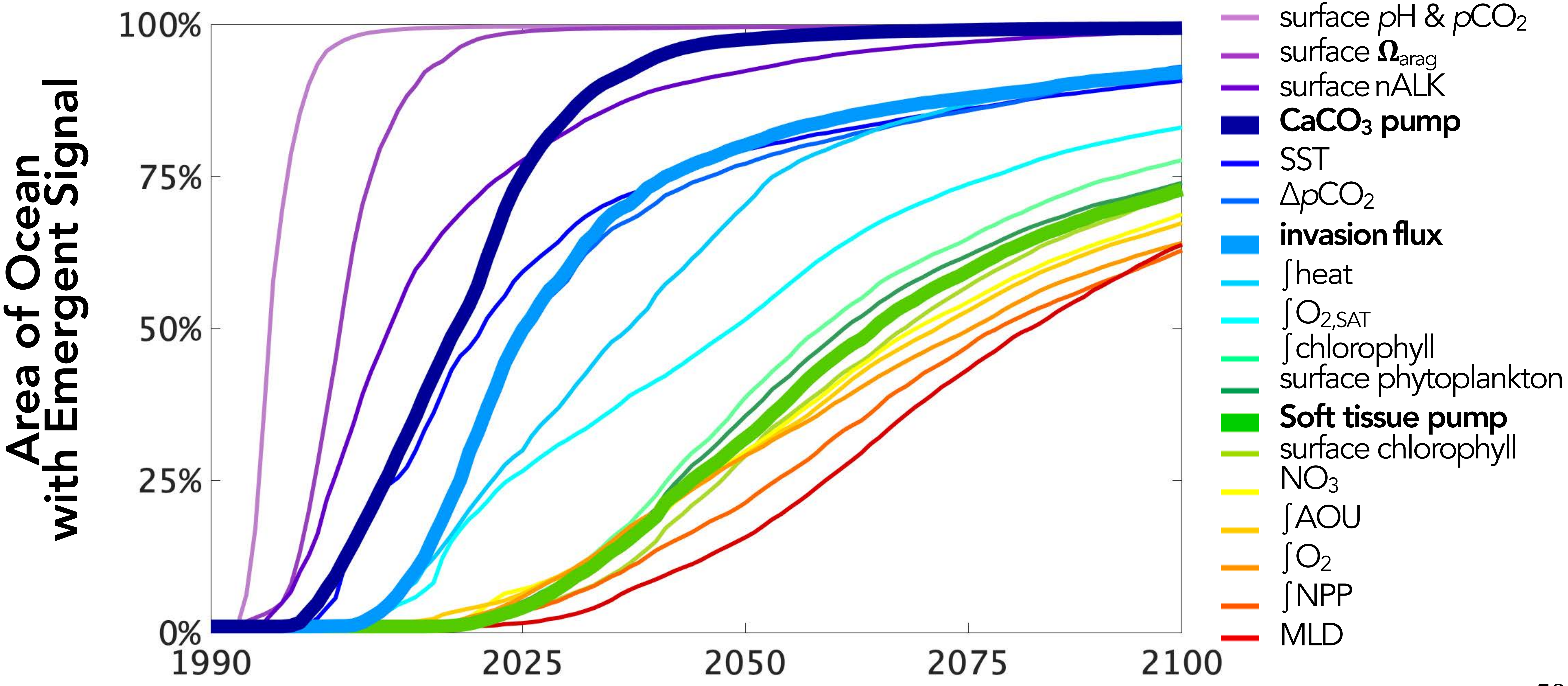

Figure 3.2: Global and regional year of emergence

	Global	Arctic Nof65N	Pacific 18N-65N	Pacific 18S-18N	Pacific 44S-18S	Atlantic 18N-65N	Atlantic 18S-18N	Atlantic 44S-18S	Indian Nof0N	Indian 44S-0N	Southern Ocean Sof45S	50% grid-cells emerged
*p*H & *p*CO_2	4	5	5	6	5	5	7	6	6	6	3	8
Ω	3	3	3	12	3	3	4	5	4	3	5	16
nALK	5	7	11	12	7	9	14	10	16	8	11	22
$CaCO_3$ export	10	14	11	18	14	13	15	12	16	18	9	30
SST	11	12	15	16	12	23	14	13	12	11	111+	33
ΔpCO_2	17	26	29	23	26	16	29	20	23	24	16	38
Air-Sea CO_2 flux	14	19	26	24	19	13	23	18	21	18	17	38
$\int$Heat	4	25	18	26	25	19	18	13	25	14	31	50
$\int O_{2,SAT}$	14	60	33	35	60	33	21	17	50	18	28	63
$\int$chlorophyll	17	52	22	31	52	41	26	84	26	36	31	72
phyto biomass	18	47	41	30	47	28	26	65	33	50	57	75
POC export	23	51	40	34	51	33	27	85	32	50	39	78
surf. chlorophyll	25	84	47	52	84	44	30	75	53	68	34	82
NO_3	24	111+	60	32	111+	20	32	36	53	50	76	84
$\int$AOU	111+	102	25	80	102	82	53	51	111+	111+	31	86
$\int O_2$	17	111+	20	111+	111+	79	55	41	106	101	27	90
$\int$NPP	36	111+	53	76	111+	103	50	45	81	111+	111+	94
MLD	38	64	22	111+	64	27	65	39	41	65	84	97
mean of all variables	22	51	27	41	51	33	29	36	40	43	41	

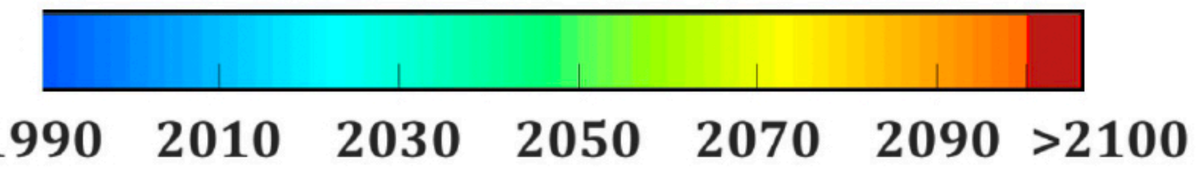

Global and regional year of emergence(after 1990) for globally- and regionally-integrated anthropogenic signals and 50% of local anthropogenic signals for the given biogeochemical variables. For each domain a single domain-averaged or domain-integrated timeseries for each variable is used to compute ToE. Color of each cell corresponds to the emergence year. Dashed boxes around the 3 ocean carbon pumps. Variables same as defined in caption of Figure 3.1

Figure 3.4: Seasonality of ΔpCO_2 ToE and Signals

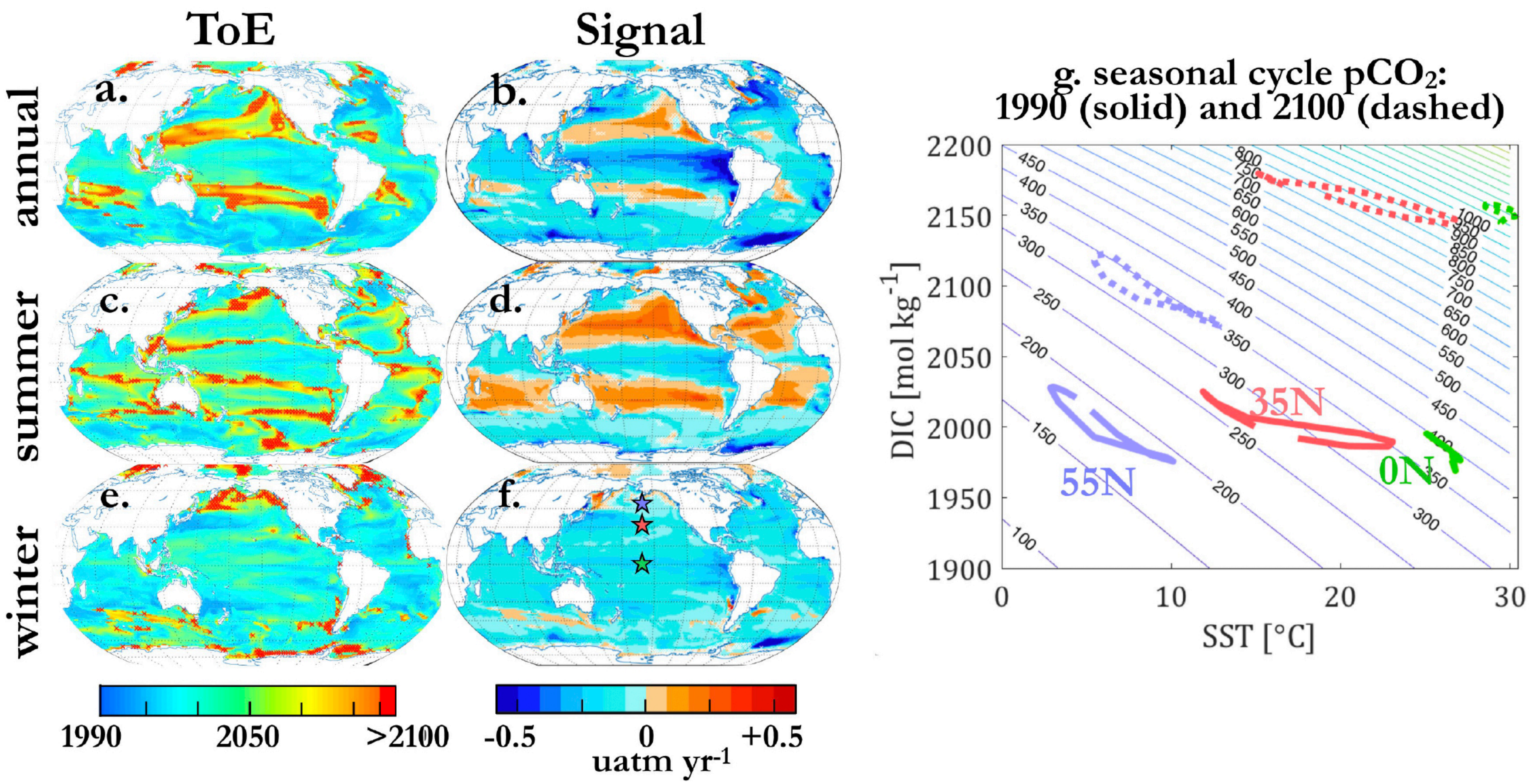

Time of Emergence for (5a.) annual (5c.) local summer and (5e.) local winter trends in sea-air ΔpCO_2 and the corresponding trend (signals) in same order (5b, d, f). July-September and January-March define summer and winter. Signals are the linear trend between 1990 and the ToE for each grid-cell. Panel 5g. shows the ensemble mean seasonal cycle of ΔpCO_2 at 3 locations along 160W (marked in 4f.) for year 1990 (solid) and year 2100 (dashed). The amplification of the seasonal pCO_2 cycle is shown on the maps and on the diagram of the season cycle at the 3 locations.

Figure 3.5: ToE and Signal Maps for surface vs. depth-integrated chlorophyll

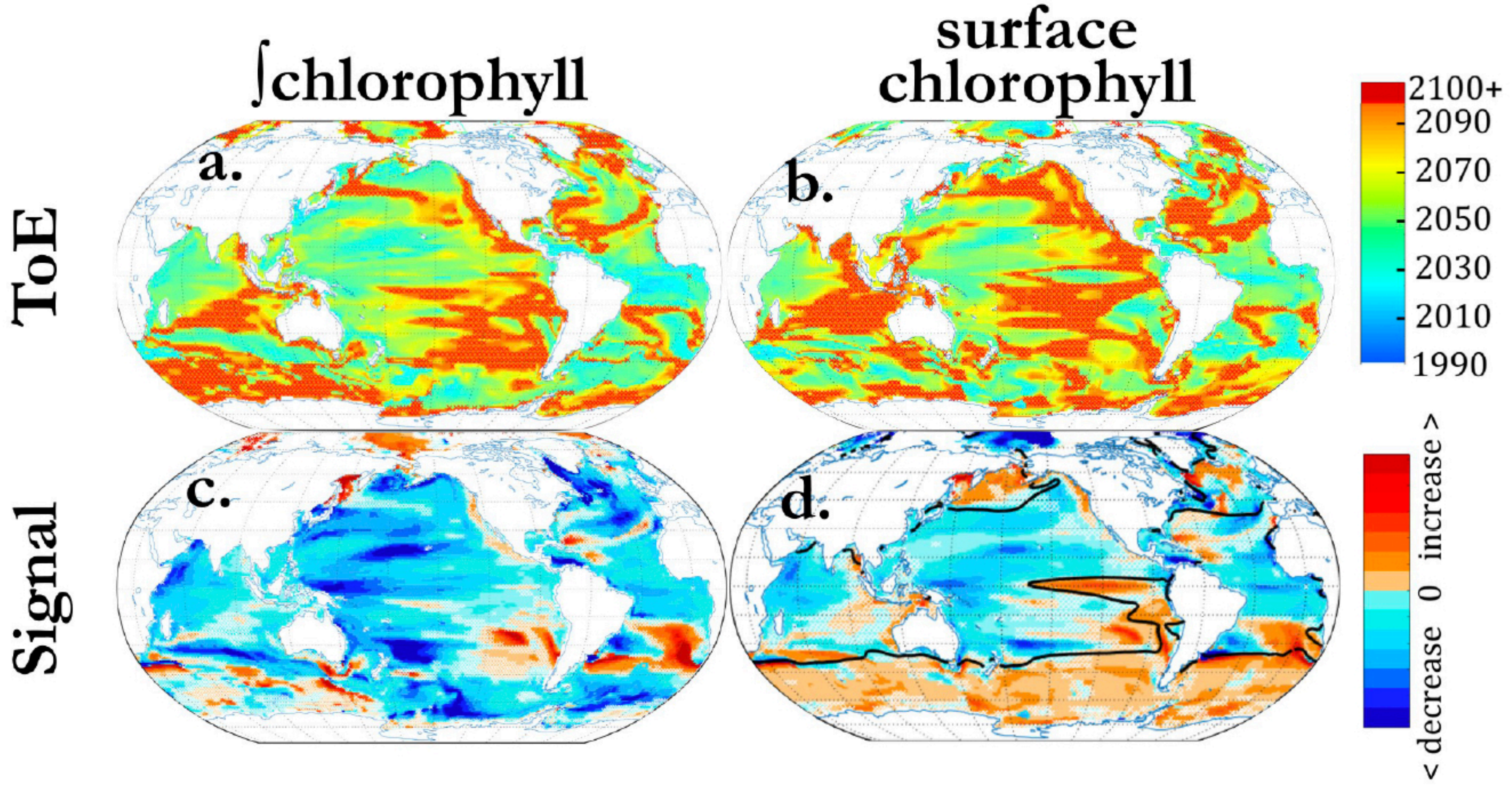

ToE (a-b) and Signal Maps (d-e) for surface vs. depth-integrated chlorophyll. Surface trends are two orders of magnitude greater than depth integrated (0-500m) trends, however emergence of integrated chlorophyll is generally earlier due to the noise reduction that occurs with depth integration. The maximum on the color scale for chlorophyll inventory signal is [$4x10^{-5}$ mmol m^{-3} yr^{-1}] and for surface chlorophyll is [$2.3x10^{-3}$ $mmol^{-3}$ yr^{-1}]. [NO_3] = 0.5 μmol kg^{-1} contours imposed on panel d.

Figure A.1: Changes in ocean carbon pumps for the LE and sensitivity experiments

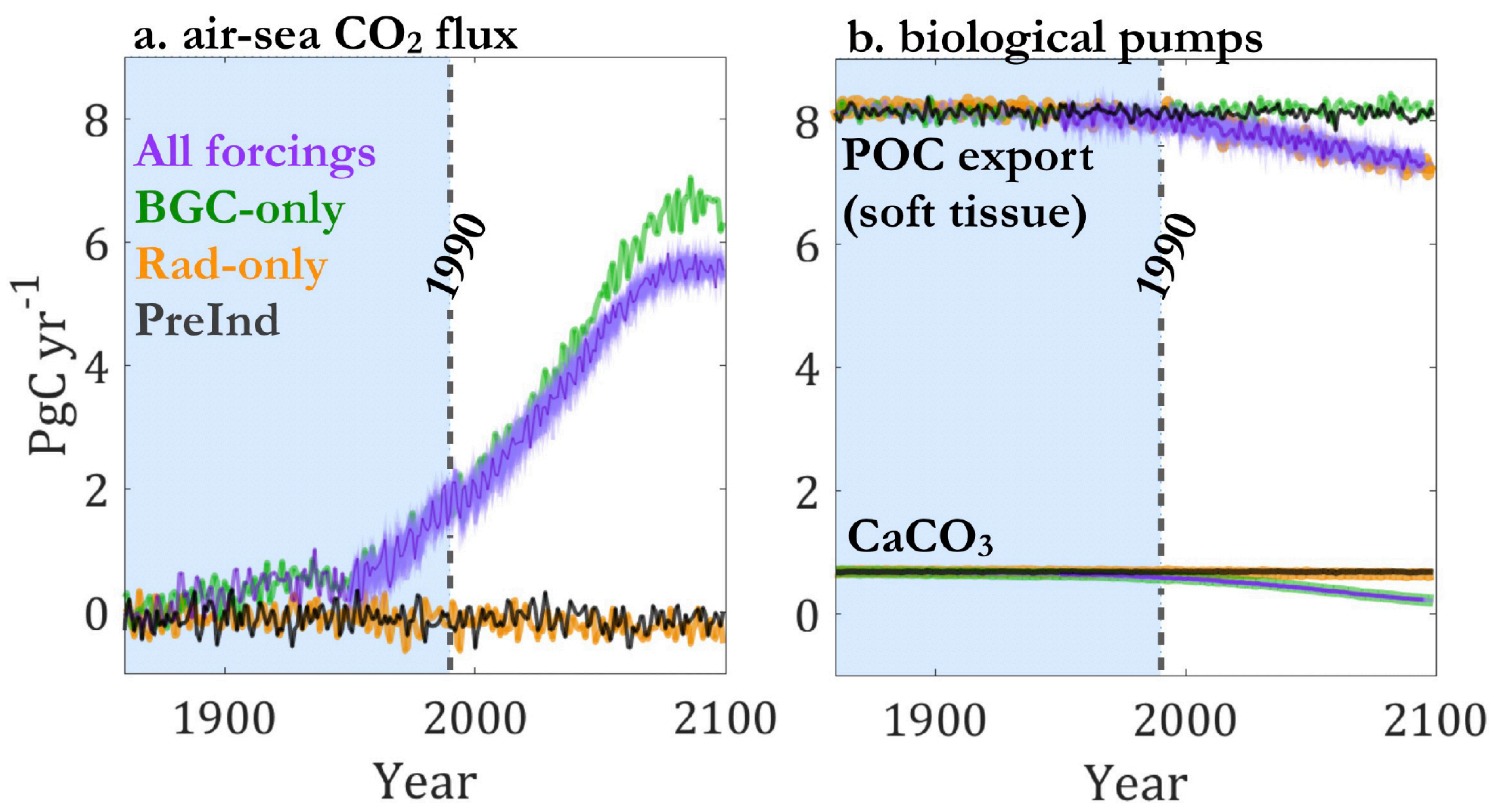

Panel a. shows the physical pump (air-sea CO_2 fluxes) and panel b the biological pumps, where POC is particulate organic carbon. Values from the sensitivity experiments are shown in different colors. All forcings indicates a fully coupled, transient run in which the forcing follows a historical to RCP8.5 pathway. In 1950, ensembles 2-29 branch from ensemble member 1, with the ensemble mean shown in darker purple. The Rad-only run includes only the radiative impacts of anthropogenic forcings, and air-sea gas exchange is not affected by rising atmospheric CO_2. The BGC-only run has only the chemical impacts of anthropogenic warming (i.e. increased CO_2 gas exchange, but no warming). PreInd indicates the pre-industrial control run. End of blue shading and dashed line at 1990 indicates the beginning of the ocean observation era, and the reference state from which emergence is defined for this paper.

Figure A.2: Change in surface ocean pCO_2 due to biological export of carbon

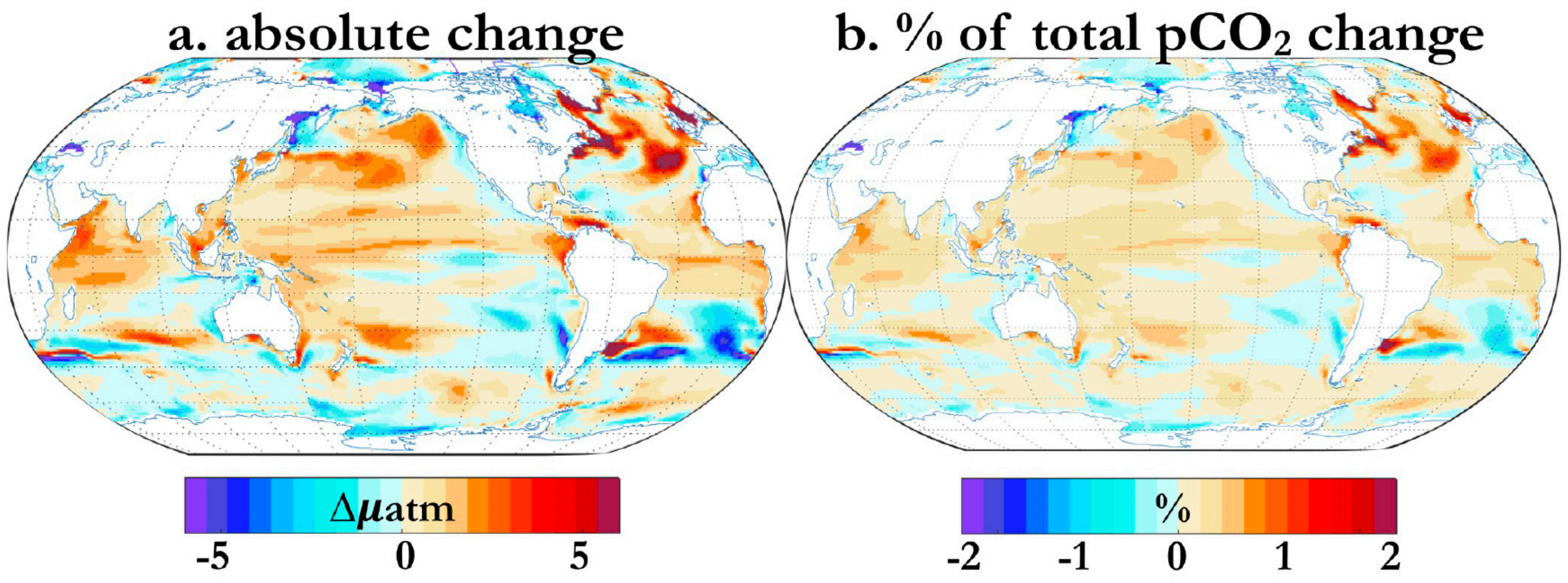

The export of soft tissue and calcium carbonate impacts surface ocean pCO_2 through changes in the concentration of alkalinity (ALK) and dissolved inorganic carbon (DIC). The impacts are not explicitly diagnosed in ESM2M, however we do offline calculations with CO2SYS (van Heuven et al., 2011) to estimate the impact of changing export on surface pCO_2. This is done by first computing pCO_2 using monthly output from the year 2100, then adjusting the concentration of DIC and ALK to account for changes in the pumps relative to 1990, and recalculating surface pCO_2 with the export-adjusted DIC and ALK concentrations. The difference between the pCO_2 at 2100 and the pCO_2 at 2100 if the pumps were stationary since 1990, is shown below. The annual mean is taken after the computations of pCO_2 are done monthly. For reference, the total pCO_2 changes by $\sim$550 uatm over this same time period, due to rising atmospheric pCO_2 and a warming surface ocean.

Figure A.7: Error for ToE calculation with Pre-Industrial noise.

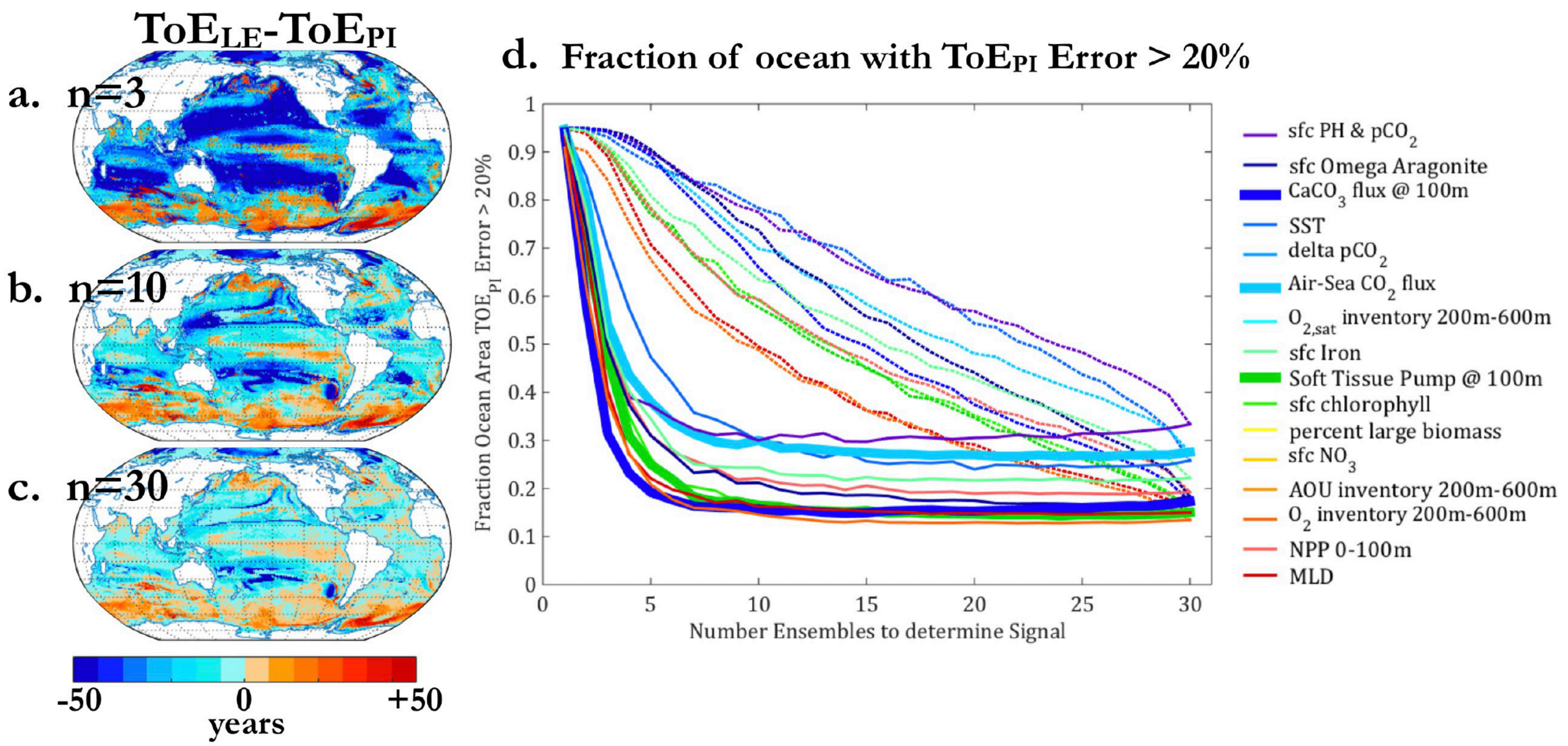

Error for ToE calculation when using Pre-Industrial noise instead of contemporary noise derrived from the LE. (a), (b), and (c) show the maximum difference between emergence times calculated for air-sea CO_2 fluxes between using the full ensemble for both signal and noise estimates (ToE_{LE}) and using pre-industrial noise (ToE_{PI}) and 3, 10 and all 30 ensemble members to estimate the anthropogenic signal. (d) shows the fractional ocean area with a difference between ToE_{LE} and ToE_{PI} greater than 20%. Increasing the number of ensemble members reduces error, however persistent error remains (∼15-30% of the globe), due to the inaccuracy of pre-industrial noise. Dashed lines are the maximum error in ToE estimates, solid lines are mean (expected) error, for the given number of ensemble used to estimate the anthropogenic signal.

Figure 6.1: Noise and Emergence for HadiSST and the GFDL-LE

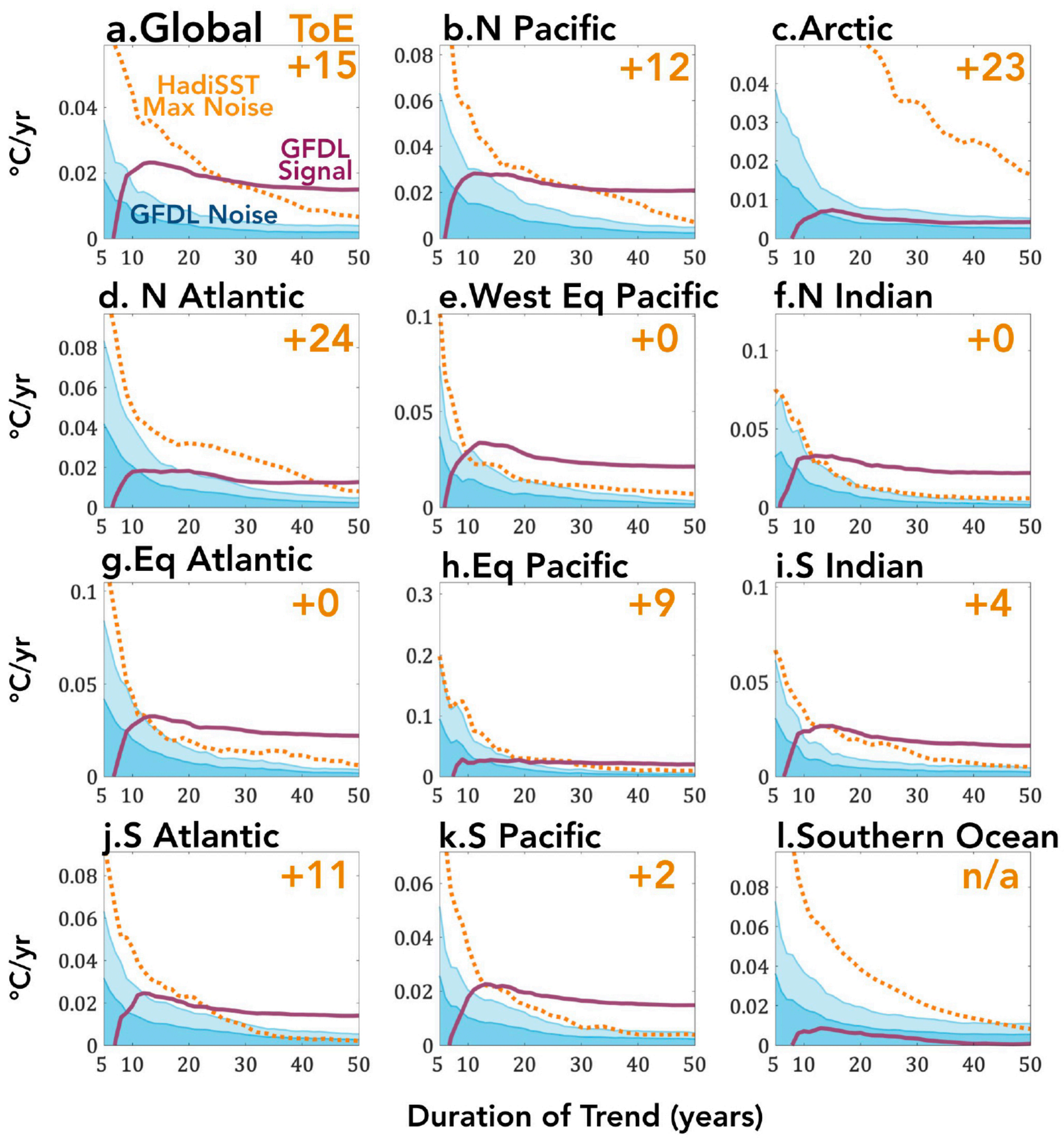

Figure 6.2: Time of Emergence using ESM Signals and HadiSST Noise

	Global	Arctic	North Pacific	WestEq Pacific	EastEq Pac	South Pacific	North Atlantic	Eq Atlantic	South Atlantic	North Indian	South Indian	Southern Ocean *
ToE_{LE} (4-model-mean)	12	39	16	14	18	15	25	15	14	13	14	23
ToE_{LE+OBS} (4-model-mean) uses HadiSST noise	26	66	26	14	34	22	28	15	17	17	14	48
difference TOE_{LE+OBS} minus TOE_{LE}	14	27	10	0	16	7	3	0	3	4	0	25

Global and regional emergence times for the mean of the 4 LEs using method presented in Chapter 2 (row 1), for the case in which HadiSST noise is used for each LE in place of model-generated noise (row 2) and the difference between the model-only vs. model-obs ToE estimates (row 3). For each LE, ToE is first computed separately before the multi-model mean is taken.